

**JOULE HEATING OF CARBON FIBERS AND THEIR COMPOSITES IN RADIO
FREQUENCY FIELDS**

A Thesis

by

SMITA SHIVRAJ DASARI

Submitted to the Graduate and Professional School of
Texas A&M University
in partial fulfillment of the requirements for the degree of

MASTER OF SCIENCE

Chair of Committee,	Micah J. Green
Committee Members,	Mustafa Akbulut
	Mohammad Naraghi
Head of Department,	Victor Ugaz

May 2023

Major Subject: Chemical Engineering

Copyright 2023 Smita Shivraj Dasari

ABSTRACT

Carbon fibers (CFs) show the ability to generate heat when exposed to radio frequency (RF) fields, but little is known about the relationship between material properties and the heating behavior. Our group has previously shown that this heating response can be used for the manufacturing of CF-reinforced composites. Here we analyze the effect of electrical conductivity on the RF-induced Joule heating patterns of CFs. Unidirectional CF tows and their composites show different heating rates when their orientations relative to the RF field lines are changed due to their anisotropic conductivities. We observed that the CFs and their composites showed higher heating responses when they were placed perpendicular to the RF field lines. We observed an increase in the heating response with increasing conductivity; however, beyond a certain conductivity value, the heating response decreases because the samples with very high conductivities reflect the RF field. We also simulated the RF-induced heating of unidirectional CF tows in different orientations, with qualitative agreement between experimental results and simulations. The findings of this work explain the effect of electrical conductivity on field-induced Joule heating of carbon fibers; these results pave the way for energy efficient, out-of-oven processing of thermoset composites at an industrial scale.

ACKNOWLEDGEMENTS

I want to express my sincere gratitude to my committee chair and advisor, Dr. Micah Green, who has been a great idol and support over the past two years. Dr. Green has mentored me throughout my time at Texas A & M University, as a researcher and a graduate student. I consider myself lucky to have gotten the opportunity to work under his esteemed guidance. He has encouraged me to present my ideas and work even when I was unsure about them and taught me to learn from my mistakes.

I am grateful to my committee members, Dr. Mustafa Akbulut and Dr. Mohammad Naraghi, for their precious time and valuable inputs during my research in the last two years.

I want to thank my colleagues and friends at our lab, who trained me and always motivated me to do my best. I really appreciate Ashley Henley and Terah Cooper of the CHEN department for all their administrative help.

I dedicate this work to my mother Dr. Livi Alex Shivraj, my father Dr. Shivraj Dasari, and my sister Shweta, without whose support I would not have achieved any success. My parents were the ones who inspired me to never stop learning, and to value my education.

CONTRIBUTORS AND FUNDING SOURCES

This work was supported by a thesis committee consisting of Dr. Micah J. Green and Dr. Mustafa Akbulut of the Department of Chemical Engineering, and Dr. Mohammad Naraghi of the Department of Aerospace Engineering.

I would like to acknowledge that the AC conductivity measurements were carried out in the Materials Characterization Facility at Texas A&M University. I thank Dr. Spencer A. Hawkins from TRI Austin; and Dr. Mohammad Naraghi and Sevketcan Sarikaya of the Department of Aerospace Engineering at Texas A&M University for providing carbon fiber samples.

Raymond D. Mee, an undergraduate researcher of the Department of Chemical Engineering provided the simulations in this work. All other work conducted for the thesis was completed by the student independently.

NOMENCLATURE

RF	Radio frequency
CF	Carbon fiber
CFRC	Carbon fiber reinforced composite
EM	Electromagnetic fields
PAN	Polyacrylonitrile
UHM	Ultra-high modulus
HT	High tenacity
IM	Intermediate modulus
J	Current density
E*	Electric field strength
Q	Power density
σ	Anisotropic conductivity tensor

TABLE OF CONTENTS

	Page
ABSTRACT.....	ii
ACKNOWLEDGEMENTS.....	iii
CONTRIBUTORS AND FUNDING SOURCES.....	iv
NOMENCLATURE.....	v
LIST OF FIGURES.....	viii
LIST OF TABLES.....	x
1. INTRODUCTION.....	1
1.1 Importance of carbon fibers and their composites.....	1
1.2 RF induced Joule heating of carbonaceous materials.....	3
1.3 Carbon fibers and RF fields.....	4
2. MATERIALS AND METHODS.....	7
2.1 Finding reflection characteristics using VNA.....	7
2.2 RF heating of CF and CFRC samples.....	7
2.3 Preparing composites of different thicknesses.....	8
2.4 Alternating Current (AC) conductivity measurements.....	9
2.5 Simulating RF heating of CFs.....	9
3. RESULTS.....	12
3.1 Heating response of unidirectional CF tows.....	12
3.2 Effect of orientation and conductivity on heating response of CFs.....	15
3.3 Effect of matrix on heating response of CFRCs.....	17
3.4 Penetration depth of RF field.....	19
3.5 Simulations.....	22
4. SUMMARY & CONCLUSIONS.....	26

REFERENCES..... 27

APPENDIX A: OPTICAL MICROSCOPY IMAGES OF T700 AND IM7
FIBERS..... 32

APPENDIX B: RECYCLE AND REUSE OF CONTINUOUS CARBON FIBERS
FROM THERMOSET COMPOSITES USING JOULE
HEATING..... 33

LIST OF FIGURES

	Page	
Figure 1 -	(a) Schematic of experimental setup for RF induced heating of CFs. (Inset: thermal image of T700 unidirectional carbon fiber tows being heated by RF at 1 W. Image captured at 30 s.) (b) Orientation of carbon fiber tows placed perpendicular, and parallel to the field. The field lines, represented by the dashed lines, come out of the plane of the applicator (fringing-field).....	5
Figure 2 -	RF induced heating rates of (a) T700 (b) IM7 (c) T300 unidirectional tows kept perpendicular to the field. RF induced heating rates of (d) T700 (e) IM7 (f) T300 unidirectional tows kept parallel to the field. The tows were heated at 1 W across a frequency range of 1 to 200 MHz. At each frequency, the tows were heated for 1 s and allowed to cool for 13 s.....	13
Figure 3 -	S ₁₁ parameters of unidirectional IM7 and T700 carbon fiber tows, were measured as a function of frequency using VNA.....	14
Figure 4 -	(a) Comparison of maximum RF induced heating rates of different types of unidirectional carbon fiber tows. For each type of carbon fiber, the heating rates of the fibers placed perpendicular to the RF field were higher than those where the CFs were placed parallel to the field. (b) Through-plane AC conductivity of different CF tows.....	15
Figure 5 -	6-ply T700 and 8-ply IM7 unidirectional composites were heated using an RF field in different orientations at 5 W across a frequency range of 1 to 200 MHz.....	17
Figure 6 -	(a) IM7 crossweave composite heated at 5 W, (b) IM7 crossweave tow heated at 5 W.....	18
Figure 7 -	(a) Illustration of composite heating process, where the heating rates change based on the number of layers of carbon fiber tows. Only the CF layers within the penetration depth are heated by the RF field. (b) Maximum heating rate of T700 unidirectional composites perpendicular to field as a function of increasing number of layers of carbon fibers. The maximum heating rate increases as the number of CF layers increase, reaches a maximum and then decreases. (c) AC conductivity of T700 unidirectional composites with varying number of carbon fiber layers.....	19

Figure 8 - Heating rates of T700 unidirectional composites with varying number of CF layers, as a function of frequency. The composites were placed perpendicular to the field and heated at 5 W power for 1 s at each 1 MHz increment in frequency..... 20

Figure 9 - (a) Transverse conductivity of T700 unidirectional composites as a function of increasing CF layers (b) Maximum heating rates of T700 unidirectional composites perpendicular to field, as a function of increasing thickness..... 21

Figure 10 - Simulated temperature profiles of RF heating at 180 MHz of T700 unidirectional tows. The temperature bar on the right shows the temperature in °C. The images are taken at 3 s of heating at 30 W when the tows are kept perpendicular to the RF field..... 23

Figure 11 - Simulated heating rates of unidirectional T700 tows at 30 W as a function of conductivity when tows are kept in different orientations (a) parallel (b) perpendicular. The conductivity on x-axis represents conductivity of bulk sample measured in the direction of the RF field. (c) Heating rates as a function of frequency at 30 W. σ_L is longitudinal conductivity and σ_T is transverse conductivity. (d) Simulated temperature profile of RF heating of T700 unidirectional tow at 30 W, captured at 3 s. The tow is oriented perpendicular to the field..... 24

LIST OF TABLES

	Page
Table 1 - Simulation parameters used in COMSOL Multiphysics 5.2 to describe the system and sample. The simulation includes the sample, the surrounding air, and the fringing-field applicator.....	10

1. INTRODUCTION

1.1 Importance of carbon fibers and their composites

Carbon fibers (CFs) have a remarkable combination of properties which make them extremely versatile [1, 2]. These materials have high tensile strength, high modulus, low density, high temperature resistance, and good electrical conductivity. Carbon fibers are made from pyrolyzing a suitable precursor material and contain at least 90% carbon by weight. Typically, most organic polymers are considered candidates for the production of carbon fibers. As long as the polymers leave a carbon residue upon thermal annealing and do not melt when heated in an inert environment, they can be used as carbon fiber precursors.

One of the most popular precursors used in the synthesis of carbon fiber is poly-acrylonitrile (PAN), which offers high tensile strength and greater elastic modulus. Polyacrylonitrile is the most common carbon-fiber precursor because PAN derived CFs have an impressive combination of tensile and compressive properties. PAN precursors also produce a high CF yield. PAN fibers were created by DuPont initially for use as textile fiber in the 1940s. Soon after, its thermal stability was discovered, which prompted more research into PAN fiber heat treatment. PAN precursors are used to create various industrial grades of carbon fibers, including high tenacity (HT) fibers, intermediate modulus (IM) fibers, high modulus (HM) fibers, and ultra-high modulus (UHM) fibers. The PAN fibers are first stabilized in air, carbonized, and graphitized in an inert environment[3]. Varying the processing parameters such as temperature during any of these steps results in different grades of carbon fibers. In this work, we have focused only on IM fibers.

Carbon fibers are often infiltrated with a polymer matrix to make carbon fiber reinforced composites (CFRCs) [4-6]. These polymers could be thermosetting epoxies or thermoplastics. In thermosetting epoxies, heat causes crosslinking or ‘curing’ of the monomer resin. For applications

in the manufacturing industry, partially cured carbon fiber composites, called ‘prepregs’, are employed; these prepregs can then be molded into the desired shape and cured completely to make large functional structures [7, 8].

Carbon fibers and CFRCs have applications in the aerospace, automobile, energy storage, and electromagnetic interference shielding industries [9-12]. PAN-based carbon fibers have been employed as the main components of energy conversion and Li-ion batteries. The carbon fiber market has been steadily expanding in recent years to keep up with demand from a variety of sectors, the military, turbine blades, construction (non-structural and structural systems), light weight cylinders and pressure vessels, offshore tethers and drilling risers, medical, automotive, sporting goods, etc. Fiber reinforced polymeric composites offer less weight and better styling for the car sector. Body pieces (doors, hoods, deck lids, front end, bumpers, etc.), chassis and suspension systems (such as leaf springs), drive shafts, and other components can all benefit from the use of carbon fiber.

Conventionally, the heating methods used in CFRC manufacturing include using ovens, hot presses, or large autoclaves [13-15]. However, these methods are time- and energy-consuming [16]. While using ovens to manufacture CFRCs, first the oven must be pre-heated to the desired temperature, and then after the CFRC is cured, additional time is required to cool the oven. Novel methods to heat and cure these polymers that surround the carbon fibers are currently being explored[17].

1.2 RF induced Joule heating of carbonaceous materials

In recent years, our group has demonstrated that certain materials (including CFs) can couple with electromagnetic (EM) fields, which cause them to heat rapidly [18, 19]. Advanced manufacturing and processing of materials can harness the ability of these materials to heat in electromagnetic fields. Electromagnetic fields can be used for targeted, non-contact, non-invasive, and material-selective heating [20, 21]. Carbonaceous nanomaterials function as susceptors and heat in response to direct current electric fields and radio frequency (RF) fields [22, 23]. RF-induced Joule heating of carbon susceptors has been used for applications including actuators [24], adhesives [25], manufacturing carbon nanotube composite materials [26], curing pre-ceramic polymer composites [27], additive manufacturing of thermoset nanocomposites [28, 29], and reduction of graphene oxide [30]. Joule heating of carbon fibers using direct current has recently been used to recycle carbon fibers from end-of-life composites[31].

Radio frequency fields have been shown to induce heating in carbon fibers in frequency ranges as low as 1-200 MHz. Carbon fibers heating in RF fields can be used to cure surrounding epoxy and fabricate carbon fiber composites without using conventional ovens. The composites are heated and cured volumetrically from the inside to the out. Previously, continuous CF/epoxy pre-pregs with controlled degrees of cross linking were manufactured using RF heating [32]. CFRCs fabricated using out-of-oven RF heating showed similar mechanical properties (like tensile strength and inter-layer lap shear strength) to composites processed using conventional methods[33].

In RF-induced Joule heating, an electric field applicator is needed to apply RF fields to the materials. In our RF setup, the applicator is made up of two metallic electrodes, one of which is

grounded and coupled to a signal generator that produces a sinusoidal RF signal. There are many different heating configurations possible with these applicators because they can couple RF fields with the sample in either a direct-contact or a non-contact way. Non-contact RF applicators we often use in our group include fringing-field and parallel plate setups. In a fringing-field applicator, the RF field curves outside the plane of the applicator. The applicator used in this work is made of copper electrodes etched onto an FR4 substrate. The geometry of the electrodes can be altered to optimize the heating efficiency.

In our prior work of RF induced heating of nanomaterials and their composites, a generalized heating pattern across a wide range of nanomaterial-loaded materials showed that the heating rates varied non-monotonically with the bulk conductivity of the material [34]. Thin films of carbon nanotubes, carbon nanofibers, and laser-induced graphene were heated using a fringing field RF applicator, and their surface conductivity was measured using a four-point probe. It was observed that at higher nanomaterial concentrations the field was reflected which resulted in a lower heating response. High nanomaterial concentrations lead to high surface conductivities. High conductivity prevents electric fields from penetrating the material, which lowers the percentage of RF fields that are absorbed, maximizing reflections. As a result, for a given frequency, increasing conductivity increases RF energy absorption only up to an optimum conductivity.

1.3 Carbon fibers and RF fields

Although several studies and uses of RF induced heating of CFs have been explored, the effect of the properties of the CFs on their heating response is not known. In principle, RF-induced heating of any material depends on its dielectric properties. Finding a relation between the electrical conductivity of CFs and their heating rates is challenging because individual CFs, arrays of CFs

(called tows), and CFRCs (both unidirectional and biaxial) are highly anisotropic. CFs' electrical and thermal conductivities are higher along their axis, compared to the radial direction [35]. A similar trend is observed for carbon fiber tows and CFRCs. In carbon fiber tows, transverse conductivity arises due to lateral contact between the individual fibers. In CFRCs, bulk transverse conductivity depends on the lateral contact between the fibers in the tow, and the dielectric properties of the matrix.

Anisotropy in individual carbon fibers is caused due to the alignment of the turbostratic carbon planes that make up the structure of a carbon fiber. Degree of anisotropy is usually a consequence of fiber processing parameters, such as temperature of heat treatment prior to carbonization, and speed of fiber drawing [36-38].

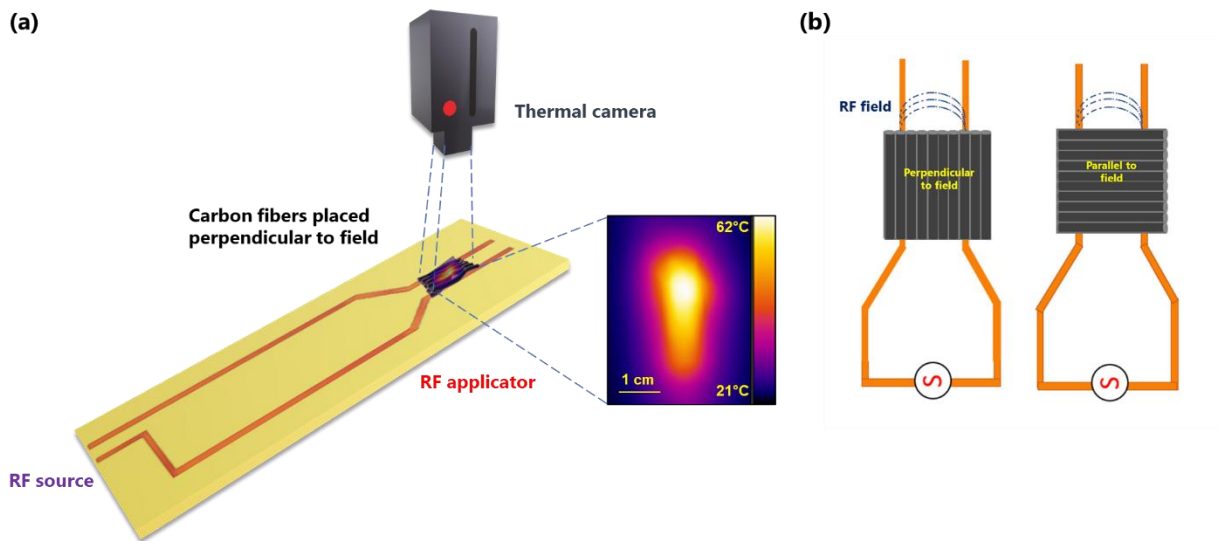


Figure 1: (a) Schematic of experimental setup for RF induced heating of CFs. (Inset: thermal image of T700 unidirectional carbon fiber tows being heated by RF at 1 W. Image captured at 30 s.) (b) Orientation of carbon fiber tows placed perpendicular, and parallel to the field. The field lines, represented by the dashed lines, extend out of the plane of the applicator (fringing-field).[39]

In this work we explore how macroscopic anisotropic fillers (such as carbon fibers) heat in RF fields and analyze their heating patterns as a function of orientation and conductivity. The macroscopic nature of these fibers makes it challenging to analyze the materials as a single bulk system. In this work, carbon fibers of varying electrical conductivities were heated in a low frequency RF field, and their heating behaviors were compared. A fringing field RF applicator and an infrared thermal camera were used to heat the carbon fiber samples and record their behavior respectively, as shown in **Figure 1**. The sample and the applicator exhibit an RLC resonance circuit-like behavior. Electrically, the two copper traces act like inductors (L). The tiny air gap between the two traces acts as a capacitor (C). The sample modifies the gap capacitance and adds a shunt resistance (R). It is observed that the heating rates of carbon fibers vary non-monotonically with their electrical conductivities.

It is important to analyze the heating rates of composites as well because carbon fibers are typically used in industry in the form of composites. In the RF heating of composites, it is essential to observe the effect of the matrix. Here, we have compared heating rates of tows and composites, and also measured how the heating behavior of composites varies with increasing thickness. Additionally, we have explored whether the heating pattern is generalizable to all types of carbon fibers and can be predicted by simulation. In simulations, we have varied the conductivity of the carbon fiber samples, to observe whether carbon fibers show a similar response to RF fields as carbon nanomaterials.

2. MATERIALS AND METHODS

IM7 unidirectional tows and IM7 cross-weave mats were purchased from Hexcel. T700SC-12K-50C and T300 unidirectional tows were purchased from Toray. 3300 epoxy and hardener were purchased from Fiberglast. T700 fibers impregnated with EPON 862 (Hexion) + Epikure W (Miller-Stephenson, Danbury, CT) curing agent resulting in 6 ply composites, IM7 fibers impregnated with EPON 862 + Epikure W curing agent resulting in 8 ply composites were used.

2.1 Finding reflection characteristics using VNA

A Vector Network Analyzer (VNA) (SVA1015X, Siglent Technologies) was used to find the reflection coefficient (S_{11}) characteristics of the bare applicator, and the different CF samples (sample under test) placed on the applicator when placed in different orientations.

2.2 RF heating of CF and CFRC samples

Every carbon fiber sample was heated in an RF field by keeping them at the same location on a fringing field RF applicator. The design of the applicator was made to ensure the sample heated symmetrically in the x- direction, and most efficiently using the RF field. We initially carried out experiments altering the angle of the fibers with respect to the axis of the applicator. We found that the maximum heating was observed when the sample was perpendicular to field, and minimum when parallel to the field. Thus, the samples were placed in two different orientations: parallel to the RF field and perpendicular to the RF field, as shown in **Figure 1**. Unidirectional tow or mat samples were heated at 1 W, while composites were heated at 5 W.

The fringing-field applicator received RF power through a 50 Ohm coaxial cable from a signal generator (Rigol Inc., DSG815) and a 500 W amplifier (Prana R&D, GN500D). A FLIR infrared

camera (FLIR Systems Inc., A655sc) was used to record the temperature, from the top of the sample, as a function of time when the sample was placed on the applicator. The signal generator was programmed with a stepwise frequency sweep to generate frequency-dependent heating rates at a fixed power in the range of 1-200 MHz. The sample was heated for 1 s, allowed to cool for 13 s, before moving to the next incremental frequency step of 1 MHz. The slope of the points in the initial linear portion of the temporal plot for each frequency was calculated to determine the heating rates as a function of frequency.

2.3 Preparing composites of different thicknesses

Unidirectional CF composites of varying thicknesses were prepared, and their RF induced heating responses were recorded. 100 parts of Fiberglast 3300 Epoxy were mixed with 22 parts of hardener by hand. The unidirectional carbon fiber tow of length 2 cm and width 0.8 cm was first placed flat on a glass slide. A drop of epoxy was spread using a roller such that the carbon fibers were impregnated with the epoxy, and any excess epoxy was removed. This is the process for making a single-layer composite sample. To make a composite with two layers, another unidirectional tow of similar dimensions was placed on top of the impregnated tow such that all the fibers are aligned in the same direction, and once again a drop of epoxy was spread over the second tow. This process was repeated to make composites of increasing layers. The impregnated carbon fiber tows were then cured in the oven for 10 minutes at 140°C to obtain carbon fiber composites of different thicknesses. The thickness of the different composites was measured using vernier calipers.

2.4 Alternating Current (AC) conductivity measurements

The through-plane AC conductivities of the carbon fiber tows and composites were found using a Novocontrol Technologies dielectric spectrometer, within the frequency range of 0.1 Hz to 10 MHz. The samples were sandwiched between a 1 cm top electrode and a larger bottom electrode. Measurements were carried out at room temperature.

2.5 Simulating RF heating of CFs

By combining the *RF* and *heat transfer in solids* modules in COMSOL Multiphysics 5.2, the simulation of RF induced heating of CFs was performed. The sample, the surrounding air, and the fringing-field applicator made up the simulated geometry. It should be noted that the simulation views the carbon fiber tow as a single, macroscopic entity rather than a collection of separate carbon fibers. The parameters such as the material properties, and geometries of the applicator and sample are listed in **Table 1**. Note that the geometry of the copper strips on the applicator used to run the simulations is different from the actual geometry of the copper strips used to run the experiments.

Table 1: Simulation parameters used in COMSOL Multiphysics 5.2 to describe the system and sample. The simulation includes the sample, the surrounding air, and the fringing-field applicator.[39]

Parameter	Value
Input Power	30 W
Input Frequency for Fig S6	180 MHz
Frequency Range for Sweep	5 MHz to 300 MHz
Characteristic Impedance	50 Ohm
Carbon Fiber Density	1800 kg/m ³
Carbon Fiber Heat Capacity	752 J/kg·K
Carbon Fiber Thermal Conductivity	9.6 W/m·K
Width of CF Sample	0.0254 m
Length of CF Sample	0.0254 m
Height of CF Sample	0.001 m
Time for which RF is on	3 s
Applicator Density	1990 kg/m ³
Applicator Thermal Conductivity	0.64 W/m·K
Applicator Heat Capacity	1550 J/kg·K

The volumetric heat source in the sample is defined by Equation 1,

$$Q = \frac{1}{2} \text{Re}(\mathbf{J} \cdot \mathbf{E}^*) \quad (1)$$

where Q is the power density in W m^{-3} , where \mathbf{J} is the current density in A/m^2 , and \mathbf{E}^* is the electric field strength in V m^{-1} .

The conductivity affects the current density as given by Equation 2,

$$\mathbf{J} = \boldsymbol{\sigma} \cdot \mathbf{E}^* \quad (2)$$

where $\boldsymbol{\sigma}$ is the anisotropic conductivity tensor in S/m .

The outer boundary of the simulation environment was set to a temperature of 20 °C. The sample in the simulation environment was set to an initial temperature of 34 °C. The RF power was supplied via a lumped port and the temperature profiles of the system were solved with a series of frequencies ranging from 5 to 300 MHz. The input power used in the simulations is 30 W. The instantaneous heating rate was calculated based on the maximum temperature observed in the system. A second set of simulations was solved using a frequency of 180 MHz while varying the longitudinal conductivity from 6.7 S/cm to 6.7×10^2 S/cm. The transverse conductivity was varied proportionally to the longitudinal conductivity. The RF field is applied for 3 s at each value of conductivity. For the purpose of this study, the sample of unidirectional carbon fibers most closely resembles a tow of T700S.

3. RESULTS

3.1 Heating response of unidirectional CF tows

CFs and their composites were exposed to a fringing RF field, and their heating response was recorded using a FLIR thermal camera. **Figure 1a** shows the schematic for the RF-induced heating setup that was used to heat the CFs and their composites in this work. The frequency-dependent heating responses of unidirectional CF tows were recorded when the fibers were placed perpendicular and parallel to the fields (**Figure 1b**). The RF field lines are generated in the out-of-plane direction as shown in **Figure 1b**. Thus, any sample of CF tow or composite can be placed in two orientations: parallel to the field lines, and perpendicular to the field lines. The thermal camera records the temperature-time data from above the sample.

We varied the frequency and measured the heating rates of the bare applicator and the samples. The frequency at which impedance matching occurred (resonant frequency), maximum heating was observed. For the bare applicator, this resonant frequency is 129 MHz. When the CF sample is placed on the applicator, this resonant frequency shifts significantly (**Figure 2**). This is because the system (sample and the applicator as a whole) has a different impedance than the bare applicator. **Figure 3** shows that the minimum S_{11} parameter for the bare applicator is found at a frequency of 127 MHz using the VNA. This value is very close to the resonant frequency observed in the actual setup.

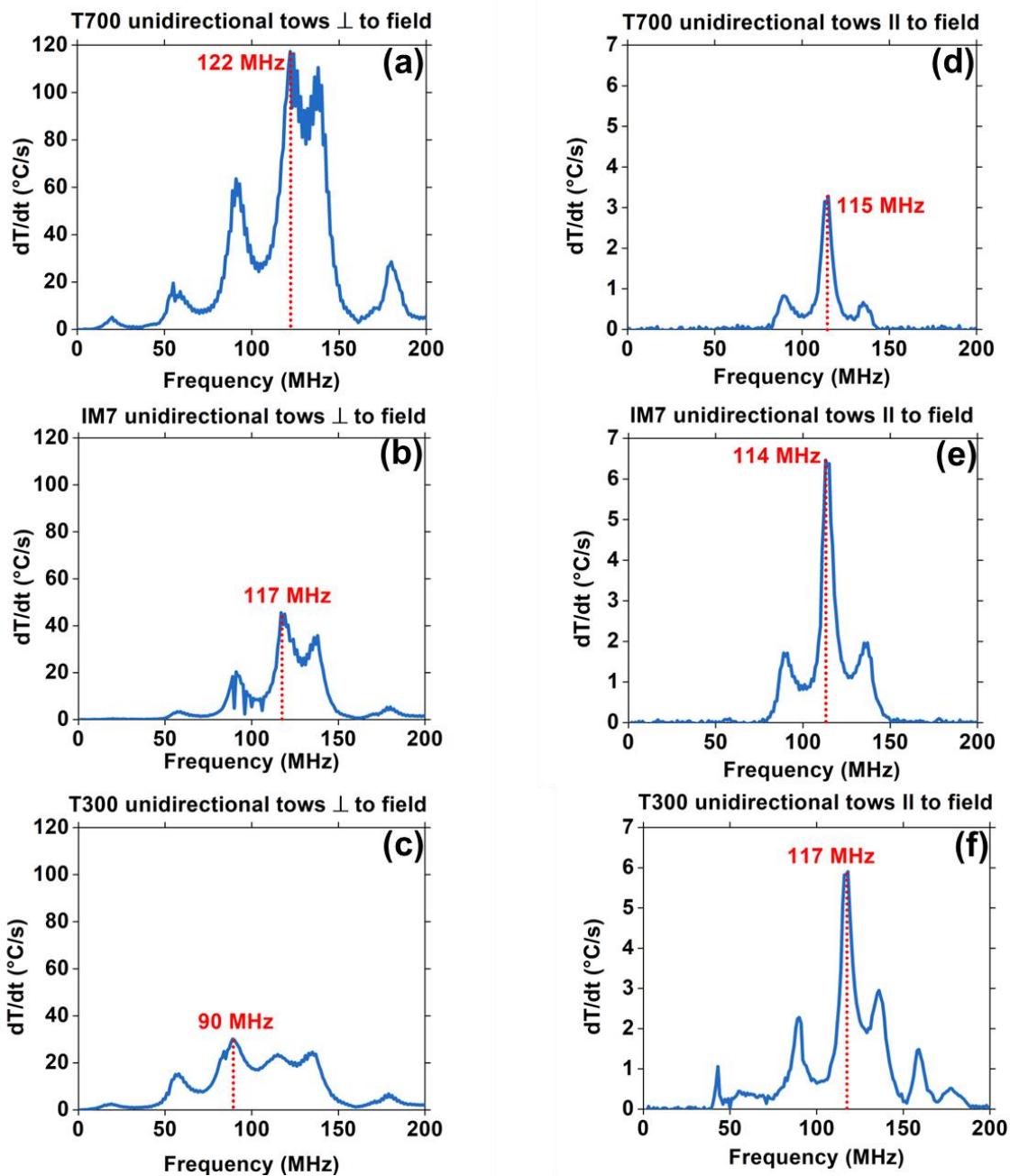


Figure 2: RF induced heating rates of (a) T700 (b) IM7 (c) T300 unidirectional tows kept perpendicular to the field. RF induced heating rates of (d) T700 (e) IM7 (f) T300 unidirectional tows kept parallel to the field. The tows were heated at 1 W across a frequency range of 1 to 200 MHz. At each frequency, the tows were heated for 1 s and allowed to cool for 13 s.[39]

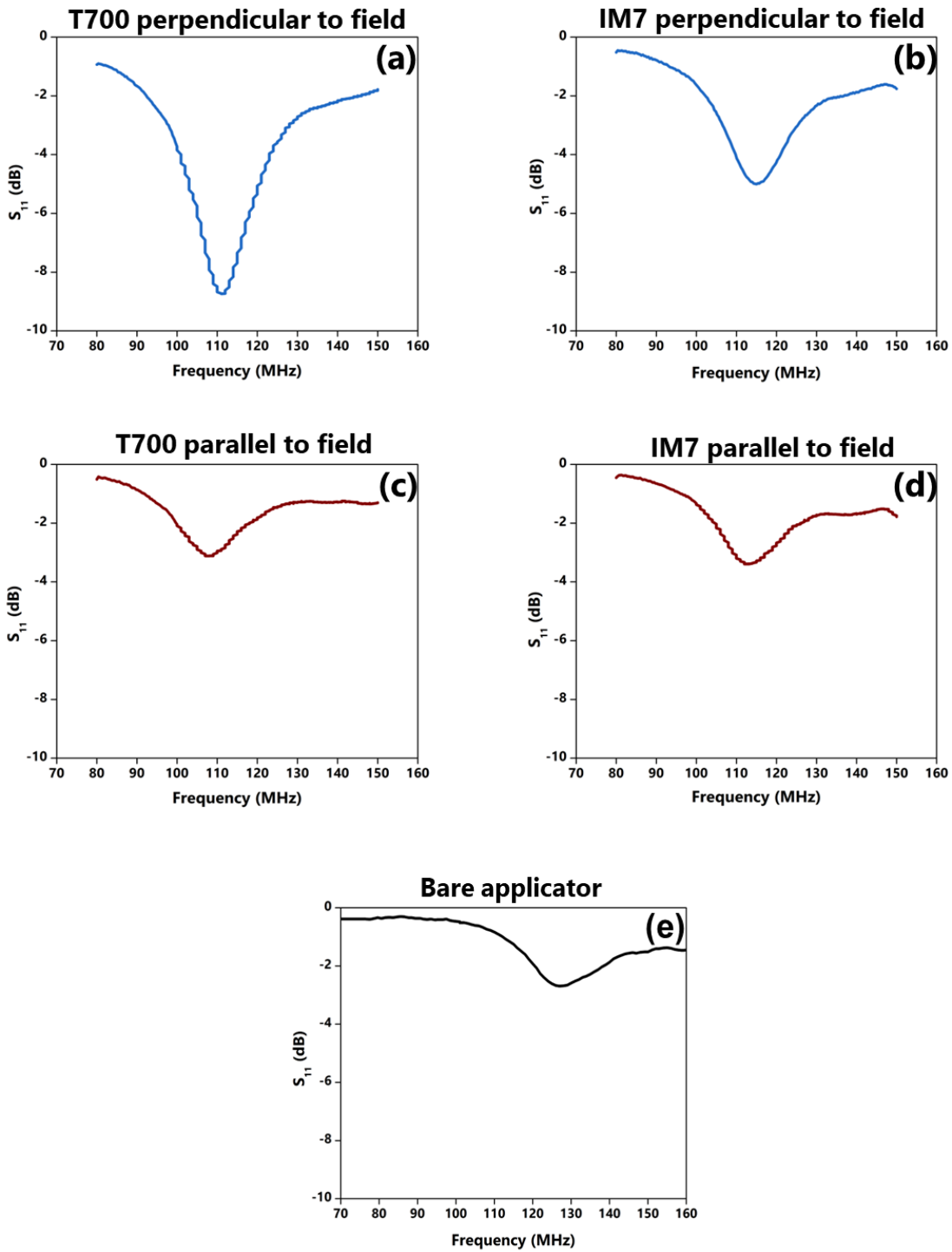


Figure 3: S_{11} parameters of unidirectional IM7 and T700 carbon fiber tows, were measured as a function of frequency using VNA.[39]

3.2 Effect of orientation and conductivity on heating response of CFs

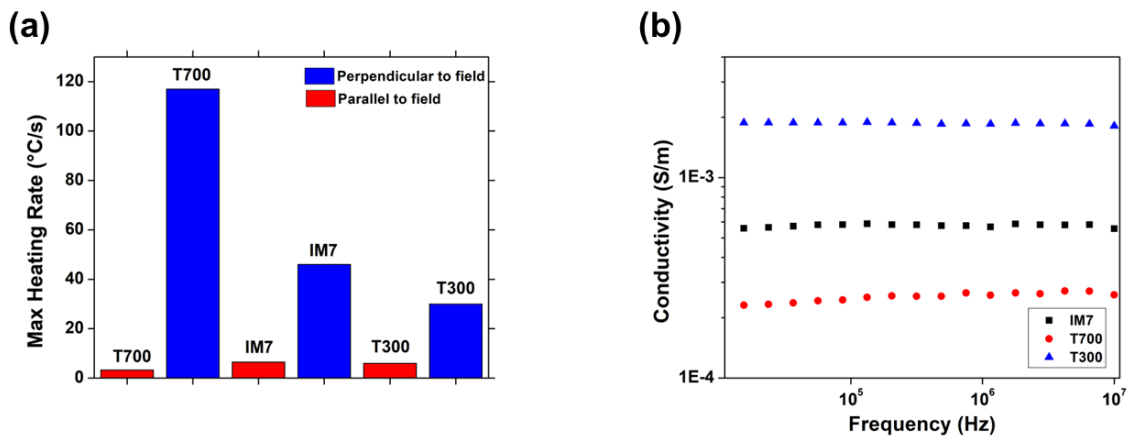


Figure 4: (a) Comparison of maximum RF induced heating rates of different types of unidirectional carbon fiber tows. For each type of carbon fiber, the heating rates of the fibers placed perpendicular to the RF field were higher than those where the CFs were placed parallel to the field. (b) Through-plane AC conductivity of different CF tows.[39]

T700, T300, and IM7 unidirectional CF tows were placed in different orientations in the RF field and their temperature-time data was recorded to compare how orientation and conductivity affected their responses. For the purpose of this research work we have compared the heating rates of three of the most commonly available standard or intermediate modulus carbon fibers that possess different longitudinal conductivities. There are multiple types of carbon fibers that are commercially available that possess different longitudinal conductivities. For instance, high modulus carbon fibers such as IM10 have a much higher longitudinal conductivity and density compared to intermediate or standard modulus carbon fibers. We expect them to show much higher heating rates when compared to IM7 or T700. **Figure 4a** shows a summary of the maximum heating rates obtained when unidirectional carbon fiber tows were heated at 1 W within a frequency range of 1 to 200 MHz in different orientations. The CFs heat up substantially more when placed perpendicular to the RF field than when placed parallel to it, irrespective of the type

of carbon fiber. We hypothesize that the heating rate of the CF sample when placed parallel to the field depends on its longitudinal conductivity, and the heating rate of the CF sample when placed perpendicular to the RF field depends on its bulk transverse conductivity.

The AC conductivities of the samples were measured using dielectric spectroscopy and are shown in **Figure 4b**. As conductivity increases, the heating rate of CF tows initially increases, reaches a maximum, and then decreases beyond a certain conductivity value; this final decrease occurs because at very high conductivity values, the reflectance of the sample increases significantly, causing the strength of the field in the system to decrease[40].

3.3 Effect of matrix on heating response of CFRCs

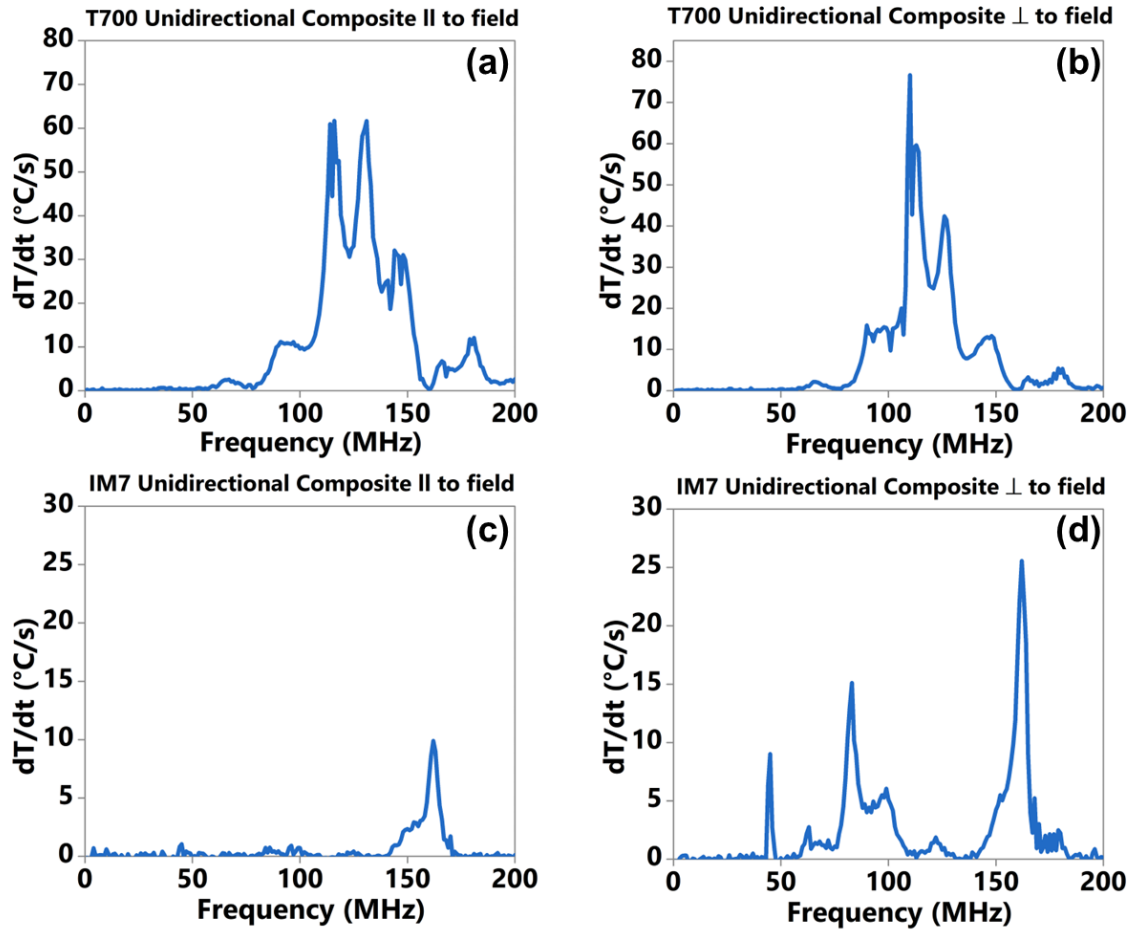


Figure 5: 6-ply T700 and 8-ply IM7 unidirectional composites were heated using an RF field in different orientations at 5 W across a frequency range of 1 to 200 MHz. The T700 composites were heated (a) parallel and (b) perpendicular to the field. The IM7 composites were heated (a) parallel and (b) perpendicular to the field.[39]

Next, the heating rates of unidirectional CF composites and tows were compared to determine the effect of the matrix. The matrix acts as an insulating layer surrounding the fibers and acts as a heat sink. In **Figure 5**, we can see that to achieve comparable maximum heating rates in composites as that of the unidirectional tows, the composites need to be heated at a higher power of 5 W. Thus, bare carbon fiber tows show significantly higher heating rates than composites. A similar

observation is made when the heating rates of IM7 crossweave tows and IM7 crossweave composites are compared in **Figure 6**. Irrespective of the number of plies of the composites, the composites show a similar trend in RF induced heating rates when placed in different orientations. Akin to unidirectional CF tows, it is observed that unidirectional CF composites heat up more when placed perpendicular to the field.

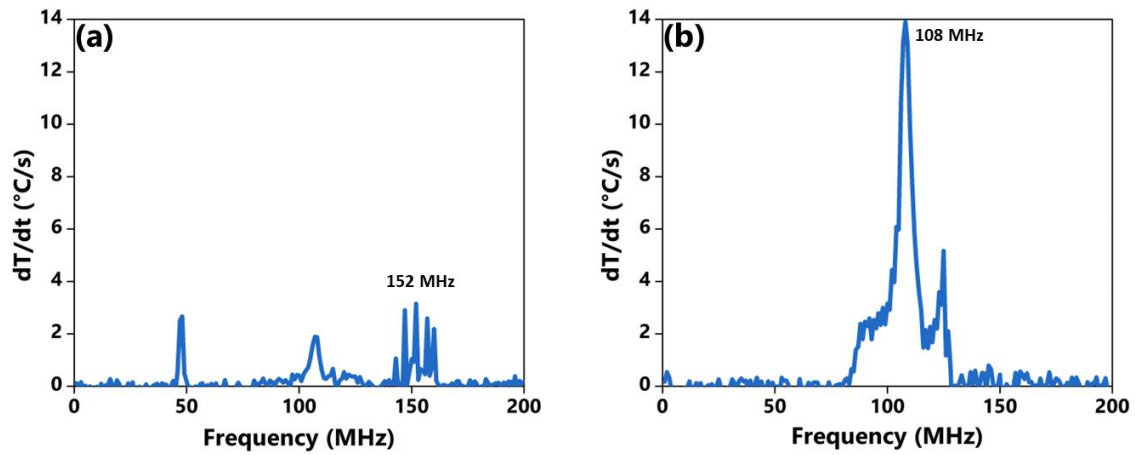


Figure 6: (a) IM7 crossweave composite heated at 5 W, (b) IM7 crossweave tow heated at 5 W.[39]

3.4 Penetration depth of RF field

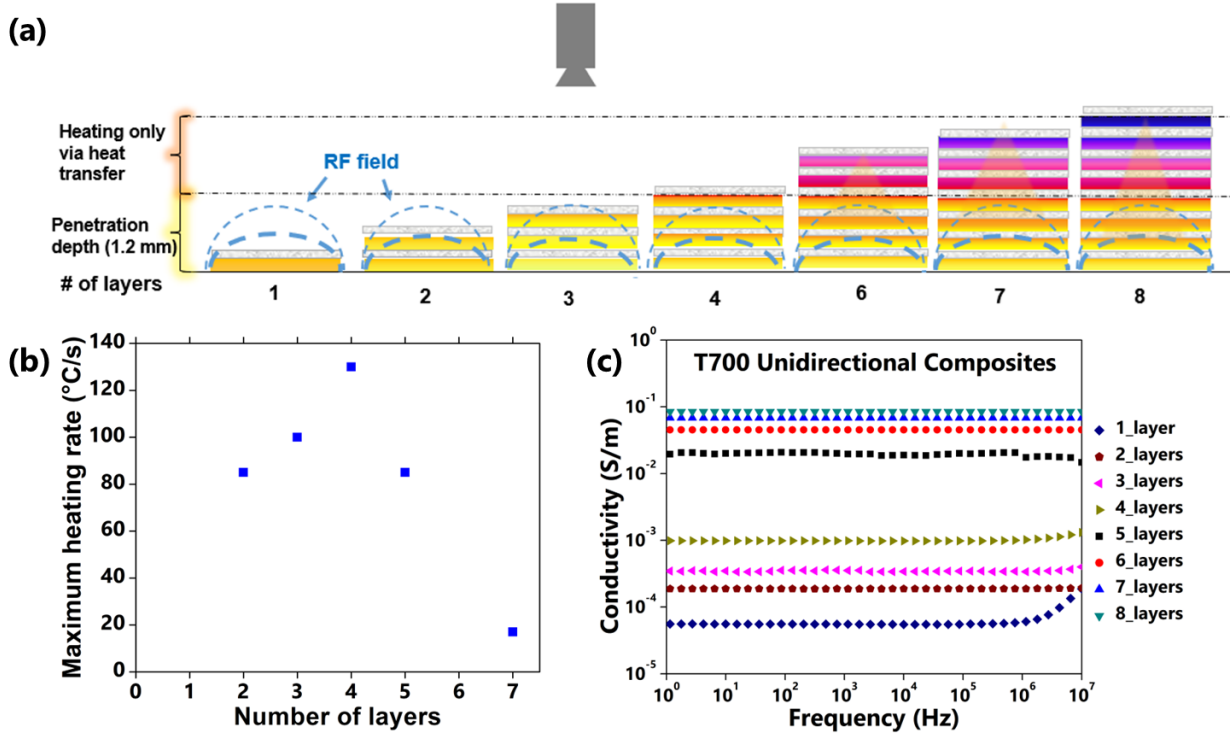


Figure 7: (a) Illustration of composite heating process, where the heating rates change based on the number of layers of carbon fiber tows. Only the CF layers within the penetration depth are heated by the RF field. (b) Maximum heating rate of T700 unidirectional composites perpendicular to field as a function of increasing number of layers of carbon fibers. The maximum heating rate increases as the number of CF layers increase, reaches a maximum and then decreases. (c) AC conductivity of T700 unidirectional composites with varying number of carbon fiber layers[39]

We hypothesize that the RF field has a certain penetration depth, beyond which the field lines do not penetrate and heat the sample (**Figure 7a**). To verify this effect of the penetration depth on the heating rates of the composites, we fabricated composites with an increasing number of CF layers.

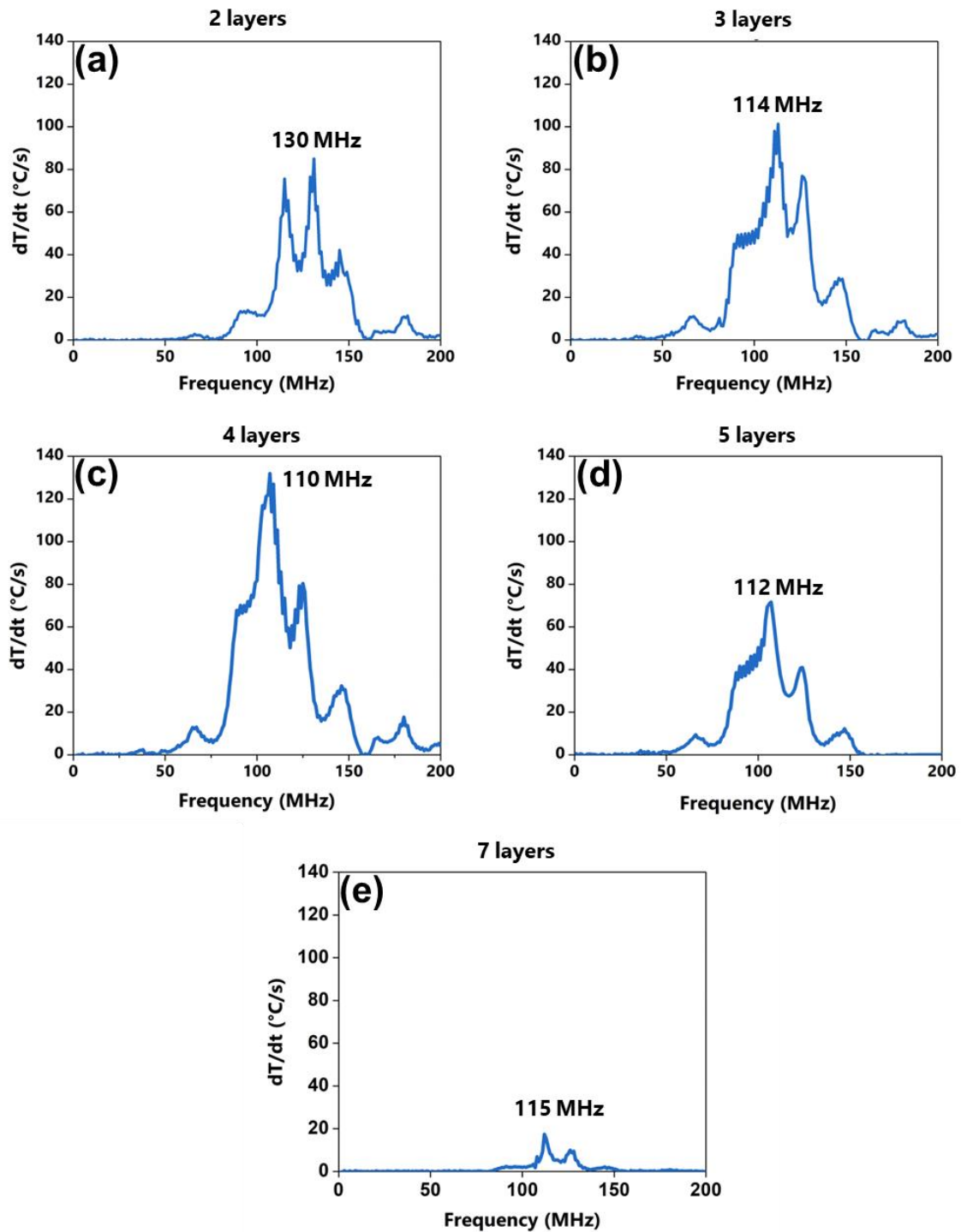


Figure 8: Heating rates of T700 unidirectional composites with varying number of CF layers, as a function of frequency. The composites were placed perpendicular to the field and heated at 5 W power for 1 s at each 1 MHz increment in frequency.[39]

Figure 7b shows that the maximum heating rates of T700 unidirectional composites increase as the number of layers increases, reaches a maximum, and then decreases. For our experimental setup the penetration depth was found to be 1.2 mm.

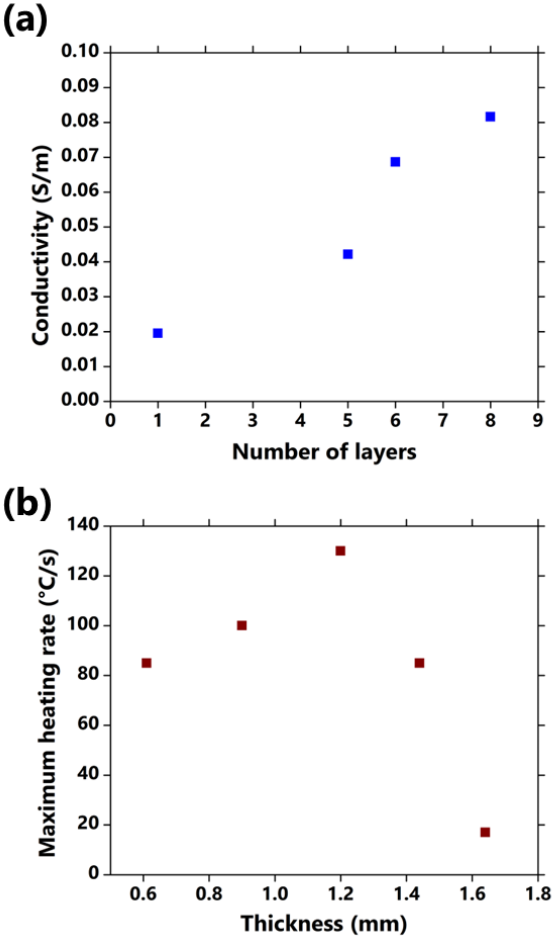


Figure 9: (a) Transverse conductivity of T700 unidirectional composites as a function of increasing CF layers (b) Maximum heating rates of T700 unidirectional composites perpendicular to field, as a function of increasing thickness[39]

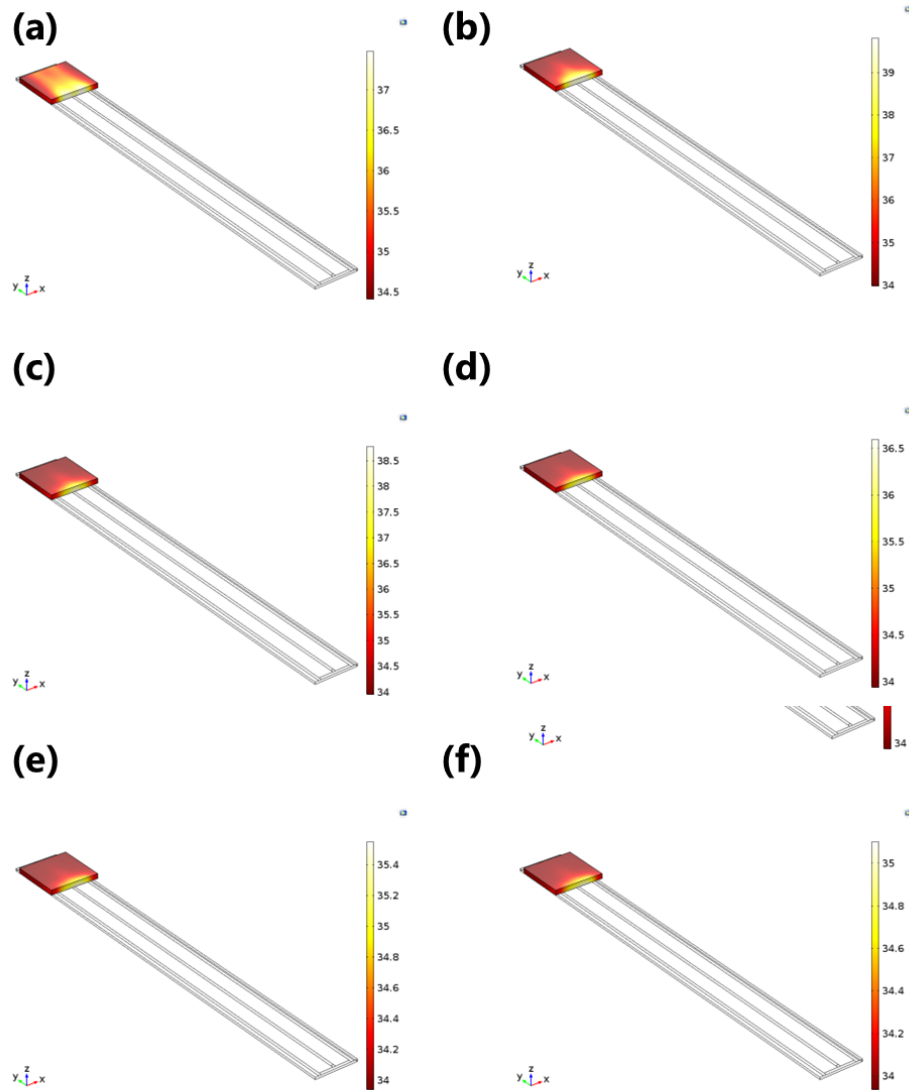
As the distance of the sample from the fringing field applicator increases, the field becomes weaker till at one point, no substantial heating is induced in the sample. Thus, no heat is generated in any of the CF layers that are outside of this penetration depth. These higher layers of CFs and epoxy

in the composites show heating only due to heat transfer from the bottom layers and not due to local heat generation, confirming our hypothesis.

As the number of carbon fiber layers increases, the bulk conductivity of the sample increases as well (**Figure 7c**). This further implies that the RF induced heating rate does increase linearly with increasing bulk conductivity of the sample. **Figure 8** displays the heating rates as a function of frequency of T700 unidirectional composites with varying number of CF layers. We can see that there is a slight shift in the frequency at which maximum heating occurs as the number of layers increases. This further adds to the notion that the sample as a whole has a particular impedance which affects its RF induced heating rate. **Figure 9** shows that the conductivity of the samples increases with increasing number of layers. It also shows how the heating rate varies with increasing thickness of these composites. The thickness of the composites increases almost linearly with increasing number of CF layers. The deviation from the linear trend occurs due to unwanted variations in pressure that occur while impregnating the composites with epoxy.

3.5 Simulations

The heating response of unidirectional CF tows were simulated using COMSOL Multiphysics to validate our experimental results. The geometry used for the simulations consisted of the sample, the surrounding air, and the fringing-field. A lumped port was used to supply the RF power, and a series of frequencies from 5 to 300 MHz were used to solve the system's temperature profiles. The frequency at which maximum heating occurs was found. Keeping this frequency (180 MHz) constant, the conductivity of the sample was varied. The simulation assumes an input power of 30 W. In the simulation, the RF field is applied only for 3 s at each value of conductivity (**Figure 10**).



Sample	(a)	(b)	(c)	(d)	(e)	(f)
Transverse Conductivity (S/m)	1	10	100	340	670	1000
Longitudinal Conductivity (S/m)	67	667	6667	22667	44667	66667

Figure 10: Simulated temperature profiles of RF heating at 180 MHz of T700 unidirectional tows. The temperature bar on the right shows the temperature in °C. The images are taken at 3 s of heating at 30 W when the tows are kept perpendicular to the RF field.[39]

Figure 11 shows simulations of how the heating rates of T700 unidirectional tows vary with conductivity when the sample is kept perpendicular to the RF field (**Figure 11a**), and parallel to the RF field (**Figure 11b**).

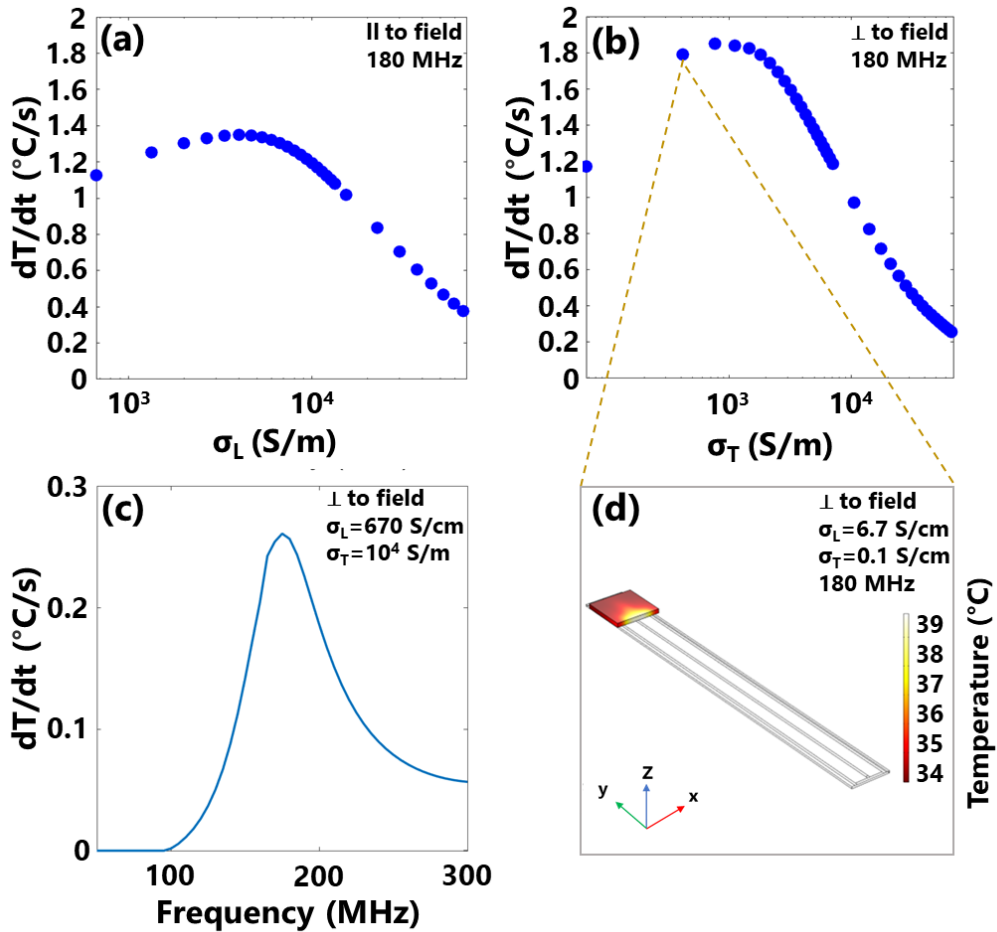


Figure 11: Simulated heating rates of unidirectional T700 tows at 30 W as a function of conductivity when tows are kept in different orientations (a) parallel (b) perpendicular. The conductivity on x-axis represents conductivity of bulk sample measured in the direction of the RF field. (c) Heating rates as a function of frequency at 30 W. σ_L is longitudinal conductivity and σ_T is transverse conductivity. (d) Simulated temperature profile of RF heating of T700 unidirectional tow at 30 W, captured at 3 s. The tow is oriented perpendicular to the field.[39]

T700S was selected as the sample to simulate the heating rates because the material properties of T700S are readily available in the literature. The conductivity values of T700S and IM7 are very

close, and it is difficult to simulate the minute differences between the different types of carbon fibers.

In the simulations we see that the heating rates of the sample when placed perpendicular to the field depend on the bulk transverse conductivity; and when placed parallel to the field, they depend on the bulk longitudinal conductivity. The simulations show that the fibers heat up more when placed perpendicular to the RF field, thus quantitatively validating the experimental results.

The simulations also show that the heating rates do not vary monotonically with the conductivity of the sample (**Figure 10**). **Figure 11c** shows that since the simulation assumes an ideal sample, only a single, clean peak is observed at the resonant frequency. The peak in the simulations is not as sharp as the experimental peaks observed at 120 MHz either. This is because the simulations do not consider the mismatch of impedance that occurs at the discontinuities within the sample. The simulation assumes a sample where the impedance is gradually changing across the frequency range, thus giving rise to a broader peak. The heating rates in the simulations are very small when compared to the experimental results. This could be attributed to the fact that (i) the simulations assume an ideal sample, applicator, and environment; and (ii) the simulations assume a uniform, bulk sample with anisotropic conductivity. However, in reality the system is more complex, and the sample is made up of distinct carbon fibers. There may be local points of resistance or electric field concentration where the carbon fibers touch each other laterally. It is remarkable that the experimental heating rates far exceed those seen in the simulations of the bulk material by a factor of almost 500. In simulations also point out that at very high conductivities, the heating rates decrease, thus implying that the field gets reflected. This is similar to what we observed in the experimental results.

4. SUMMARY & CONCLUSIONS

The heating behavior of carbon fibers and their composites when exposed to radio-frequency fields were investigated. Heating response of fibers is dependent on two major factors: electrical conductivity, and orientation of exposure to field. With rise in electrical conductivity, the heating response initially increases before reaching a maximum value, beyond which it decreases. This ultimate decrease in heating occurs because the reflectance of the RF field increases with increasing electrical conductivity of the CFs. We have also observed that the temperature distribution and efficiency of heating depends on the geometry of the RF applicator used. Unidirectional carbon fibers (and their composites) have shown faster heating rates when placed perpendicular to the RF field lines. This could be because the heating rate of the CF sample when placed parallel to the field depends on its longitudinal conductivity, and the heating rate of the CF sample when placed perpendicular to the RF field depends on its bulk transverse conductivity. As the conductivity of the sample increases significantly, its heating rate decreases. At higher conductivities, the RF field is reflected by the sample. In the case of composites, the matrix has a significantly lower electrical conductivity; thus, overall heating response is much lower compared to bare fibers. Finite Element simulations of the RF heating process were performed using COMSOL Multiphysics, and qualitatively a similar trend of heating rate as a function of sample conductivity was observed. These findings help us better understand the factors that affect the heating response of macroscopic filler composites when exposed to electromagnetic fields, which will prove useful in scaling up of manufacturing processes involving these materials.

REFERENCES

1. Figueiredo JL, Bernardo CA, Baker R, Hüttinger K: *Carbon fibers filaments and composites*. Springer Science & Business Media; 2013.
2. Yang S, Cheng Y, Xiao X, Pang H: **Development and application of carbon fiber in batteries**. *Chemical Engineering Journal* 2020, **384**:123294.
3. Minus M, Kumar S: **The processing, properties, and structure of carbon fibers**. *JOM* 2005, **57**:52-58.
4. Morgan P: *Carbon fibers and their composites*. CRC press; 2005.
5. Iwahori Y, Ishiwata S, Sumizawa T, Ishikawa T: **Mechanical properties improvements in two-phase and three-phase composites using carbon nano-fiber dispersed resin**. *Composites Part A: Applied Science and Manufacturing* 2005, **36**:1430-1439.
6. Chung D: *Carbon fiber composites*. Elsevier; 2012.
7. Marsh G: **Prepregs — raw material for high-performance composites**. *Reinforced Plastics* 2002, **46**:24-28.
8. Odagiri N, Kishi H, Yamashita M: **Development of TORAYCA prepreg P2302 carbon fiber reinforced plastic for aircraft primary structural materials**. *Advanced Composite Materials* 1996, **5**:249-254.
9. Frank E, Hermanutz F, Buchmeiser MR: **Carbon Fibers: Precursors, Manufacturing, and Properties**. *Macromolecular Materials and Engineering* 2012, **297**:493-501.
10. Newcomb BA: **Processing, structure, and properties of carbon fibers**. *Composites Part A: Applied Science and Manufacturing* 2016, **91**:262-282.
11. Geetha S, Satheesh Kumar K, Rao CR, Vijayan M, Trivedi D: **EMI shielding: Methods and materials—A review**. *Journal of applied polymer science* 2009, **112**:2073-2086.

12. Tang S, Hu C: **Design, preparation and properties of carbon fiber reinforced ultra-high temperature ceramic composites for aerospace applications: a review.** *Journal of Materials Science & Technology* 2017, **33**:117-130.
13. Chung DD: *Composite materials: science and applications.* Springer Science & Business Media; 2010.
14. Koushyar H, Alavi-Soltani S, Minaie B, Violette M: **Effects of variation in autoclave pressure, temperature, and vacuum-application time on porosity and mechanical properties of a carbon fiber/epoxy composite.** *Journal of Composite Materials* 2012, **46**:1985-2004.
15. Lucía O, Maussion P, Dede EJ, Burdío JM: **Induction Heating Technology and Its Applications: Past Developments, Current Technology, and Future Challenges.** *IEEE Transactions on Industrial Electronics* 2014, **61**:2509-2520.
16. Joseph C, Viney C: **Electrical resistance curing of carbon-fibre/epoxy composites.** *Composites Science and Technology* 2000, **60**:315-319.
17. Collinson MG, Bower MP, Swait TJ, Atkins CP, Hayes SA, Nuhiji B: **Novel composite curing methods for sustainable manufacture: A review.** *Composites Part C: Open Access* 2022, **9**:100293.
18. Wasselynck G, Trichet D, Ramdane B, Fouldagar J: **Interaction between electromagnetic field and CFRP materials: a new multiscale homogenization approach.** *IEEE Transactions on Magnetics* 2010, **46**:3277-3280.
19. Forintos N, Czigany T: **Multifunctional application of carbon fiber reinforced polymer composites: Electrical properties of the reinforcing carbon fibers—A short review.** *Composites Part B: Engineering* 2019, **162**:331-343.

20. Müller B, Palardy G, Teixeira De Freitas S, Sinke J: **Out-of-autoclave manufacturing of GLARE panels using resistance heating.** *Journal of Composite Materials* 2018, **52**:1661-1675.
21. Chien A-T, Cho S, Joshi Y, Kumar S: **Electrical conductivity and Joule heating of polyacrylonitrile/carbon nanotube composite fibers.** *Polymer* 2014, **55**:6896-6905.
22. Vashisth A, Upama ST, Anas M, Oh J-H, Patil N, Green MJ: **Radio frequency heating and material processing using carbon susceptors.** *Nanoscale Advances* 2021, **3**:5255-5264.
23. Anas M, Zhao Y, Saed MA, Ziegler KJ, Green MJ: **Radio frequency heating of metallic and semiconducting single-walled carbon nanotubes.** *Nanoscale* 2019, **11**:9617-9625.
24. Oh JH, George GW, Martinez AD, Moores LC, Green MJ: **Radio frequency heating of PEDOT:PSS.** *Polymer* 2021, **230**:124077.
25. Gruener JT, Vashisth A, Pospisil MJ, Camacho AC, Oh J-H, Sophia D, Mastroianni SE, Auvil TJ, Green MJ: **Local heating and curing of carbon nanocomposite adhesives using radio frequencies.** *Journal of Manufacturing Processes* 2020, **58**:436-442.
26. Sweeney CB, Moran AG, Gruener JT, Strasser AM, Pospisil MJ, Saed MA, Green MJ: **Radio Frequency Heating of Carbon Nanotube Composite Materials.** *ACS Applied Materials & Interfaces* 2018, **10**:27252-27259.
27. Patil N, Zhao X, Mishra NK, Saed MA, Radovic M, Green MJ: **Rapid Heating of Silicon Carbide Fibers under Radio Frequency Fields and Application in Curing Preceramic Polymer Composites.** *ACS Applied Materials & Interfaces* 2019, **11**:46132-46139.

28. Sarmah A, Desai SK, Tezel GB, Vashisth A, Mustafa MM, Arole K, Crowley AG, Green MJ: **Rapid Manufacturing via Selective Radio-Frequency Heating and Curing of Thermosetting Resins.** 2022, **24**:2101351.
29. Sarmah A, Desai SK, Crowley AG, Zolton GC, Tezel GB, Harkin EM, Tran TQ, Arole K, Green MJ: **Additive manufacturing of nanotube-loaded thermosets via direct ink writing and radio-frequency heating and curing.** *Carbon* 2022, **200**:307-316.
30. Debnath D, Zhao X, Anas M, Kulhanek DL, Oh JH, Green MJ: **Radio frequency heating and reduction of Graphene Oxide and Graphene Oxide - Polyvinyl Alcohol Composites.** *Carbon* 2020, **169**:475-481.
31. Sarmah A, Sarikaya S, Thiem J, Upama ST, Khalfaoui AN, Dasari SS, Arole K, Hawkins SA, Naraghi M, Vashisth A, Green MJ: **Recycle and Reuse of Continuous Carbon Fibers from Thermoset Composites Using Joule Heating.** *ChemSusChem* 2022, **15**:e202200989.
32. Vashisth A, Healey RE, Pospisil MJ, Oh JH, Green MJ: **Continuous processing of pre-pregs using radio frequency heating.** *Composites Science and Technology* 2020, **195**:108211.
33. Sarmah A, Morales MA, Srivastava A, Upama S, Nandi A, Henry TC, Green MJ, Vashisth A: **Interfacial carbon fiber-matrix interactions in thermosetting composites volumetrically cured by electromagnetic fields.** *Composites Part A: Applied Science and Manufacturing* 2022:107276.
34. Anas M, Mustafa MM, Vashisth A, Barnes E, Saed MA, Moores LC, Green MJ: **Universal patterns of radio-frequency heating in nanomaterial-loaded structures.** *Applied Materials Today* 2021, **23**:101044.

35. Park J, Hwang T, Kim H, Doh Y: **Experimental and numerical study of the electrical anisotropy in unidirectional carbon-fiber-reinforced polymer composites.** *Smart materials and structures* 2006, **16**:57.
36. Fitzer E, Frohs W, Heine M: **Optimization of stabilization and carbonization treatment of PAN fibres and structural characterization of the resulting carbon fibres.** *Carbon* 1986, **24**:387-395.
37. Ji X, Matsuo S, Sottos NR, Cahill DG: **Anisotropic thermal and electrical conductivities of individual polyacrylonitrile-based carbon fibers.** *Carbon* 2022, **197**:1-9.
38. Tse-Hao K, Tzy-Chin D, Jeng-An P, Ming-Fong L: **The characterization of PAN-based carbon fibers developed by two-stage continuous carbonization.** *Carbon* 1993, **31**:765-771.
39. Dasari SS, Sarmah A, Mee RD, Khalfaoui AN, Green MJ: **Joule Heating of Carbon Fibers and Their Composites in Radio-Frequency Fields.** *Advanced Engineering Materials*, **n/a**:2201631.
40. Anas M, Zhao Y, Saed M, Ziegler K, Green M: **Radio Frequency Heating of Metallic and Semiconducting Single-Walled Carbon Nanotubes.** *Nanoscale* 2019, **11**.

APPENDIX A

OPTICAL MICROSCOPY IMAGES OF T700 AND IM7 FIBERS



Figure A6: Optical microscopy image of T700 to measure its radius.

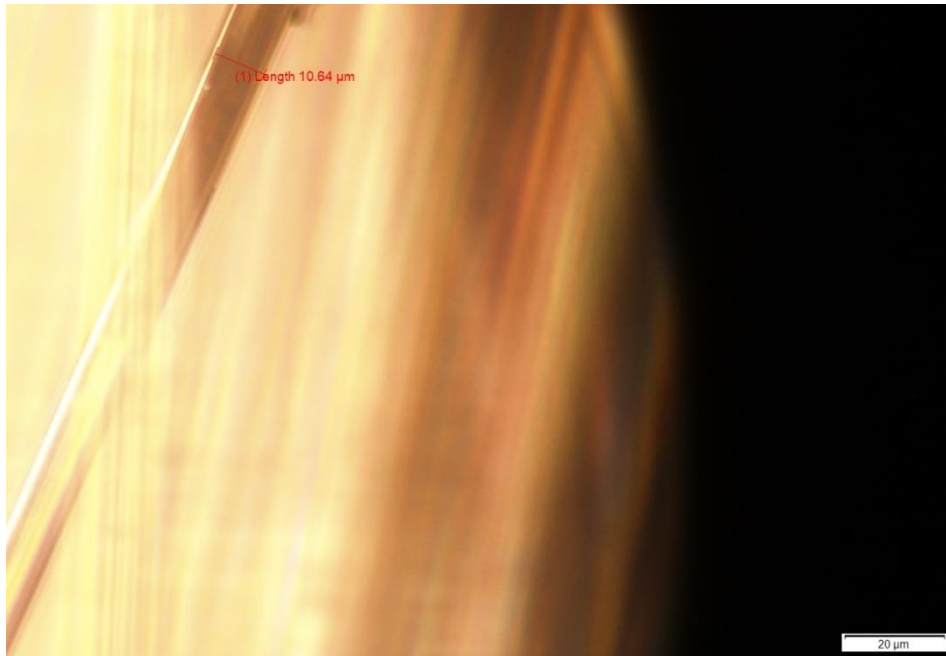


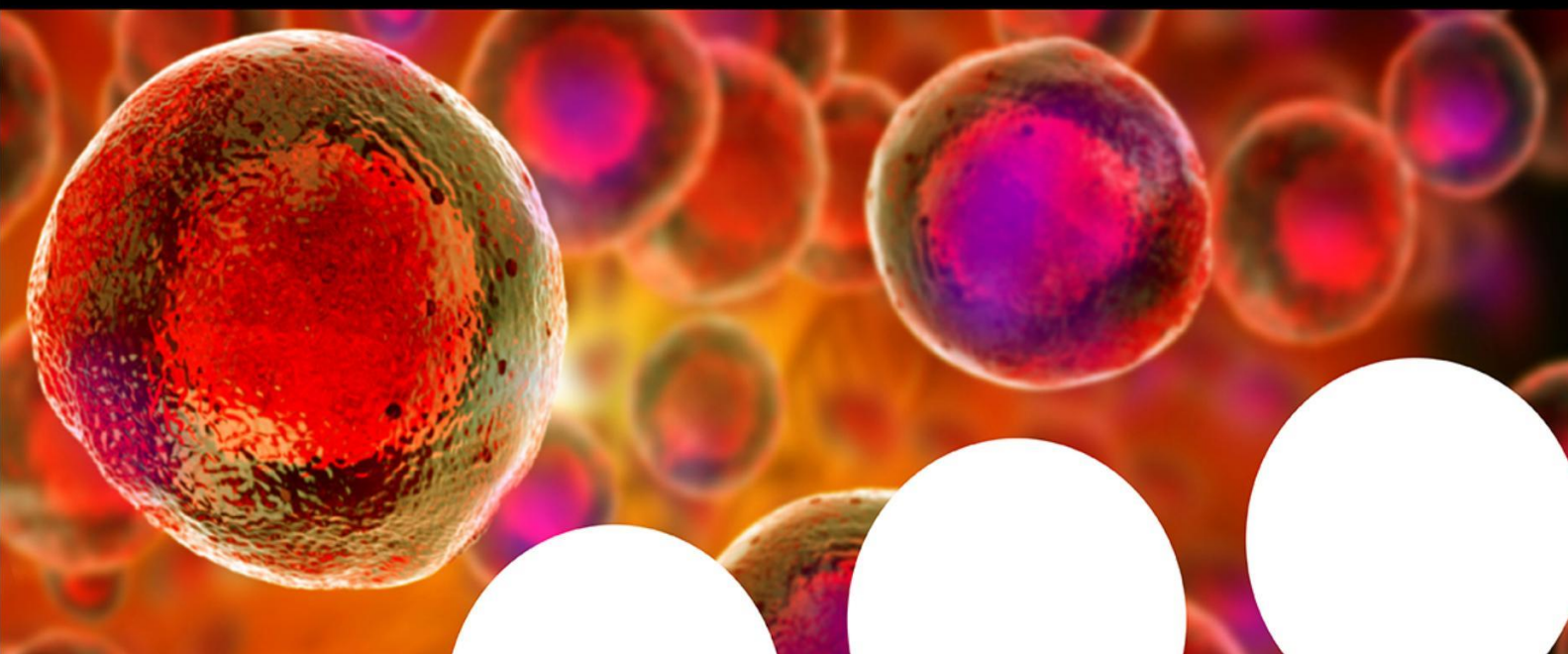
Figure A7: Optical microscopy image of IM7 to measure its radius.

APPENDIX B

RECYCLE AND REUSE OF CONTINUOUS CARBON FIBERS FROM THERMOSET COMPOSITES USING JOULE HEATING

In collaboration with Anubhav Sarmah of our lab group, I worked on the Joule heating of carbon fibers to recycle T700 continuous carbon fibers from thermoset composites. This work gave me an understanding of the applications of volumetric heating of CFs when they interact with electric fields. Our work entitled 'Recycle and Reuse of Continuous Carbon Fibers from Thermoset Composites Using Joule Heating' (shown below) was published in the Journal 'ChemSusChem' in August 2022.

Your research is important and needs to be shared with the world



Benefit from the Chemistry Europe Open Access Advantage

- Articles published open access have higher readership
- Articles are cited more often than comparable subscription-based articles
- All articles freely available to read, download and share.

Submit your paper today.



Recycle and Reuse of Continuous Carbon Fibers from Thermoset Composites Using Joule Heating

Anubhav Sarmah,^[a] Sevetcan Sarikaya,^[b] Jonathan Thiem,^[c] Shegufta T. Upama,^[b] Aida N. Khalfaoui,^[a] Smita Shivraj Dasari,^[a] Kailash Arole,^[b] Spencer A. Hawkins,^[d] Mohammad Naraghi,^[b, e] Aniruddh Vashisth,^[c] and Micah J. Green^{*[a, b]}

This study demonstrates a new and sustainable methodology for recycling continuous carbon fibers from end-of-life thermoset composite parts using Joule heating. This process addresses the longstanding challenge of efficiently recovering carbon fibers from composite scrap and reusing them to make fresh composites. The conductive carbon fibers volumetrically heat up when an electric current is passed through them, which in turn rapidly heats up the surrounding matrix sufficiently to degrade it. Fibers can be easily separated from the degraded matrix after the direct current (DC) heating process. Fibers reclaimed using this method were characterized to determine their tensile properties and surface chemistry, and compared against both as-received fibers and fibers recycled using

conventional oven pyrolysis. The DC- and oven-recycled fibers yielded similar elastic modulus when compared against as-received fibers; however, an around 10–15% drop was observed in the tensile strength of fibers recycled using either method. Surface characterization showed that DC-recycled fibers and as-received fibers had similar types of functional groups. To demonstrate the reusability of recycled fibers, composites were fabricated by impregnation with epoxy resin and curing. The mechanical properties of these recycled carbon fiber composites (rCFRCs) were compared against conventional recycling methods, and similar modulus and tensile strength values were obtained. This study establishes DC heating as a scalable out-of-oven approach for recycling carbon fibers.

Introduction

Carbon fiber reinforced composites (CFRCs) have myriad applications in the military, aerospace, and automotive industries.^[1,2] Their popularity is due to the superior properties of carbon fibers, such as high tensile strength, light weight, and high modulus.^[3,4] CFRCs can be broadly classified into thermoplastic composites and thermoset composites based on the type of matrix used. Here, we focus on the specific challenge of recycling continuous carbon fibers from thermoset CFRCs.

The matrix in thermoset composites is usually the product of an irreversible crosslinking reaction;^[5] thus, it cannot be reprocessed or remolded in any way, rendering the recycling of

fibers from these parts a particularly challenging task.^[6,7] Traditionally, thermoset CFRC waste has been incinerated or disposed of in landfills.^[8] This has led to high disposal costs and negative environmental impacts.^[9] Thermoset matrices deteriorate under mechanical and thermal stresses or undergo chemical degradation with repeated use and age. On the other hand, carbon fibers remain intact because they have high thermal, chemical, and mechanical stability.^[10] Thus, carbon fibers can be recovered from end-of-life cured composites and from partially cured 'pre-preg' scraps with minimal loss in properties, so that they can be reused.^[11,12] Reusing carbon fibers also eliminates the large amount of energy required to produce virgin carbon fibers.^[11,13–15] Therefore, there is a growing need to develop a method to degrade the epoxy matrix from thermoset composites and then reclaim continuous carbon fibers.

Current techniques for deteriorating the matrix and recovering carbon fibers can be classified into mechanical methods,^[16] solvolysis,^[17] pyrolysis,^[18] and electrochemical methods.^[19] Mechanical methods include grinding and milling.^[20] These methods produce only short carbon fibers; composites made using chopped fibers are not competitive with CFRCs made from continuous fibers.^[21] In the solvolysis method, organic solvents are used to degrade the epoxy matrix. However, this process is time-consuming, and the solvents are environmentally hazardous.^[22] Supercritical fluids have also been investigated for use in solvolysis.^[23] These fluids require equipment that can withstand high pressures and temperatures, thus increasing capital costs.^[11,24] In electrochemical methods, chlorination inside an electrochemical cell degrades the epoxy matrix.^[25] Disadvantages of this method include the post-


[a] A. Sarmah, A. N. Khalfaoui, S. S. Dasari, Prof. M. J. Green
Artie McFerrin Department of Chemical Engineering
Texas A&M University
College Station, TX, 77843 (USA)
E-mail: micah.green@tam.u.edu

[b] S. Sarikaya, S. T. Upama, K. Arole, Prof. M. Naraghi, Prof. M. J. Green
Department of Materials Science & Engineering
Texas A&M University
College Station, TX, 77843 (USA)

[c] J. Thiem, Dr. A. Vashisth
Department of Mechanical Engineering
University of Washington
Seattle, WA, 98195 (USA)

[d] Dr. S. A. Hawkins
Texas Research Institute, Inc.
Austin, TX, 78746 (USA)

[e] Prof. M. Naraghi
Department of Aerospace Engineering
Texas A&M University
College Station, TX, 77843 (USA)

 Supporting information for this article is available on the WWW under <https://doi.org/10.1002/cssc.202200989>

process drying of the carbon fibers, the long process times, the requirement of large volumes of electrolytes, and the use of expensive materials such as platinum electrodes; these factors make this process difficult to scale up.^[26]

Oven pyrolysis is currently the most commonly used method for carbon fiber recycling.^[11] In this method, the matrix is decomposed in an inert environment at temperatures ranging from 350 C to 700 C.^[27–29] This process is conventionally carried out in large-scale ovens. Pyrolysis is typically followed by oxidation of the retrieved carbon fibers to remove the epoxy char on the surface of the fibers.^[11] The entire process, including oxidation, requires a minimum of about 30 min for a sample size of 250 g.^[30] Another method that uses high temperatures for carbon fiber recycling is the fluidized bed process, which involves heating the CFRC composite using air between 450–550 C in a bubbling sand bed. The major drawback of the fluidized bed method is that initial continuous fibers are broken down into short and fluffy chopped fibers. Recently, using microwaves to thermally degrade the matrix has garnered attention. The microwaves heat and degrade the matrix at temperatures ranging from 450 C to 650 C, and fibers are retrieved at the end of the process.^[30,31]

The engineering community thus faces a difficult task: despite the need to recycle carbon fibers from thermoset CFRCs, the actual technology to do so remains elusive. It is highly desirable to develop a method to retrieve continuous carbon fibers from end-of-life composites without using environmentally toxic solvents and reagents.

To address this objective and avoid the problems associated with existing technologies, we propose the use of Joule heating via direct current (DC). Joule heating, or resistive heating, occurs when an electric current is passed through a conductive material. Our group has previously shown that DC heating can heat up conductive pixels for thermal patterning.^[32] Joule heating has also been successfully used to synthesize graphene fibers from graphene oxide.^[33] In another study, Joule heating was used to recover precious metals from electronic waste.^[34]

In this study, we explore a methodology for out-of-oven thermal recycling of carbon fibers from scrap composites (Figure 1). A DC voltage is applied across a CFRC using a DC power source; the conductive fibers enable a current to pass through it, heating up in the process. The hot fibers heat up the surrounding matrix, and since the degradation temperatures of fibers are much higher than that of the matrix, the process temperature can be monitored and controlled to target the matrix without affecting the fibers specifically. Fibers retrieved using this method were characterized and compared against fibers recycled using conventional oven pyrolysis; surface characteristics and fiber strength turned out to be consistent across samples degraded using the two heating methods. Next, to test the utility of the recycled fibers, we made recycled carbon fiber composites (rCFRCs) by reinfiltrating the fibers with epoxy and curing the composite; similar mechanical results were obtained for the composites made using fibers recycled via DC heating and conventional oven pyrolysis. Finally, the scalability of this method was investigated by finding a relation-

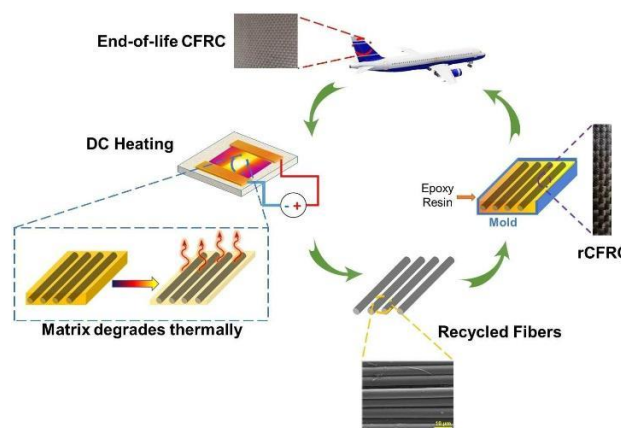


Figure 1. Schematic showing closed-loop recycling of carbon fibers from end-of-life composites using DC heating, and fabrication of recycled carbon fiber composites for industrial applications.

ship between the power required for composites of various sizes.

Results and Discussion

We first describe the DC heating process to recycle carbon fibers from composite scrap. Next, we assess the properties of DC-recycled fibers and compare them against as-received fibers and conventionally recycled fibers. Finally, we demonstrate the application of recycled fibers to fabricate rCFRCs, and compare against composites fabricated from as-received fibers.

We first determine the relevant degradation temperatures of the matrix using thermogravimetric analysis (TGA). A temperature ramp from room temperature to 600 C (in air) showed that the matrix for cross-weave and unidirectional composites used in this study degraded at around 400 C (Figure S1). Next, isothermal TGA runs in the air at 400 C showed that at the end of 10 min, the cross-weave composite had a residue of 77%, while the unidirectional composite had a residue of 55% (Figure S2). These numbers roughly correspond to the fiber to matrix weight ratio in the composite, and we aimed to achieve these ratios with our DC heating experiments.

We next demonstrate our DC heating methodology to degrade the matrix and recycle the fibers (Figure 2a). A current was allowed to pass through 4-ply thick samples of cross-weave and unidirectional composites with in-plane dimensions 1 cm × 1 cm. This allowed the conductive fibers to heat up volumetrically and transfer the heat to the surrounding resin. A temperature of 400 C (Figure S3) was maintained for about 10 min by modulating the DC voltage, based on feedback from the thermal camera; uniform heating of the sample was observed, which ensured that the matrix in the entire sample was evenly degraded. Visual observation confirmed that after the elapsed time, the matrix was eliminated, and the fibers had begun to fray and separate.

To show that this method can be scaled up to continuous composite rolls, longer composites of in-plane dimensions

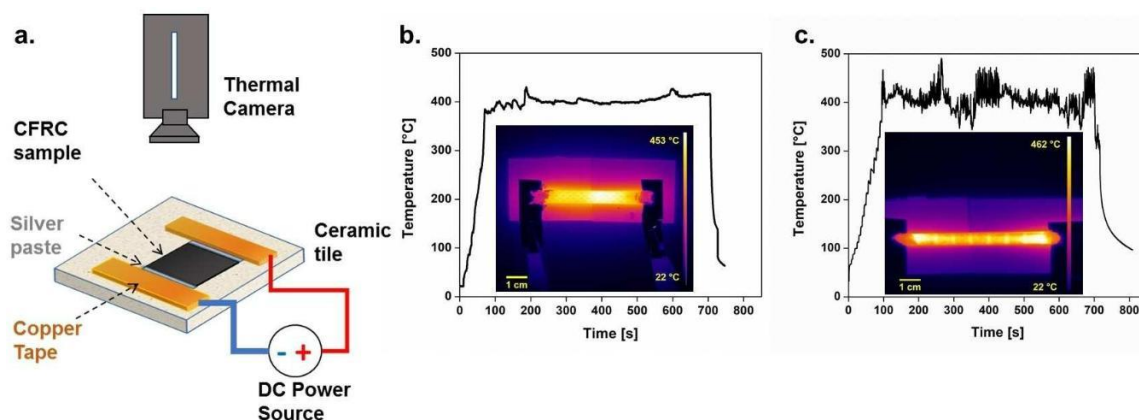


Figure 2. (a) Schematic of DC heating setup. CFRC sample (black) is placed on the ceramic tile; electrical contact is established using copper tape and conductive silver paste. The sample is connected to a DC power source using alligator clips; temperature is monitored using a thermal camera. (b) Time-temperature data (inset: thermal image from forward-looking infrared (FLIR) camera at $t=200$ s) during DC heating of cross-weaved IM7 and (c) unidirectional IM7 composite.

approximately $7\text{ cm} \times 1\text{ cm}$ were heated; the temperature was rapidly ramped up to about 400 C within a minute and maintained isothermally for 10 min (Figure 2b, c). Typical weights of the composite before and after DC heating are shown in Table S1; these weight ratios were close to the ones obtained from TGA. This shows that DC heating can be successfully used to recycle continuous carbon fibers from scrap CFRCs, without using environmentally hazardous reagents.

The surface chemistry of the recovered carbon fibers was analyzed using X-ray photoelectron spectroscopy (XPS); the XPS spectra of the carbon fibers are shown in Figure S4. The as-received carbon fibers show O and C peaks, but do not show any N peaks. These as-received fibers have a thin coating on them which enhances cross-linking between the fiber and matrix; this is called 'sizing.' The as-received fibers were thermally treated at 450 C for 15 min to remove the sizing. After removal of the sizing on the fibers, the 'de-sized' carbon fibers show N, C, and O peaks. The N peak that appears in the de-sized carbon fibers belongs to the N atoms present in the carbon fiber itself (remnants of the polyacrylonitrile-based precursor) and the amine (NH_2) functional groups. After the DC recycling process, the N peak becomes stronger compared to the de-sized carbon fiber. C, O, and N percentages for each carbon fiber are listed in Table S2. The as-received carbon fibers and de-sized carbon fibers have a slightly higher O/C ratio (21 % and 17 %, respectively) than the DC-recycled ones (12.9%). The O/C ratio quantifies the oxygen-containing functional groups on the surfaces of the carbon fibers and indicates the active surface area of chemical bonding between the carbon fibers and epoxy resin. The as-received carbon fibers and de-sized carbon fibers may have a slightly higher O/C ratio than the DC-recycled ones because de-sizing and DC recycling slightly oxidizes the surface of carbon fibers and cleaves the functional groups that contain oxygen. The functional groups on the fiber surface were determined by C 1s deconvoluted spectra. The C 1s narrow spectra were deconvoluted to show three peaks, namely C-C (284.4 eV),

C-O-C ($285.02\text{--}286.03\text{ eV}$), and O-C=O ($287.9\text{--}288.4\text{ eV}$), according to their distinguished binding energy. The results of C 1s spectra fittings of carbon fibers are shown in Figure 3a–d, and the contents of the functional groups are listed in Table S3. The same types of functional groups were found on the surfaces of recycled and as-received fibers. These functional groups help create covalent bonds between the carbon fibers and the epoxy matrix during re-impregnation. The DC-recycled carbon fibers have a noticeably higher density of hydroxyl groups and carbonyl groups compared to de-sized carbon fibers. This is likely because the DC recycling of CFRC composites leaves some functional groups from the original matrix on the surface of the carbon fibers.

The surface morphologies of as-received, DC-recycled, and oven-recycled carbon fibers were investigated via scanning electron microscopy (SEM, Figure 3e–g) and optical microscopy (Figure S5). No major damage on carbon fibers was observed in the SEM images. Also, there is very little epoxy remaining on the surface of the DC-recycled carbon fibers. This residue was removed after washing the carbon fibers in an ultrasonic bath.

Tensile testing of recycled individual carbon fibers was performed to measure the tensile strength and modulus, and to determine if their mechanical properties were altered during recycling. Fibers recycled using DC heating and oven pyrolysis have similar modulus values of around $180\text{--}190\text{ GPa}$, as shown in Figure 3h. However, we see an about 10–15% decrease in tensile strength of DC and oven-recycled fibers when compared to as-received fibers (Figure 3i). This loss in strength is consistent with previous studies which involved thermal degradation of the matrix to reclaim carbon fibers.^[31] Individual tensile test outcomes in box plot format are shown in Figure S6.

Incineration of CFRCs produces 3.39 kg of CO_2 per kg of CFRC waste. Greenhouse gas emissions associated with virgin carbon fiber production have been estimated previously at $31\text{ kg CO}_2\text{ equiv. per kg}$, which is 10 times more than conventional steel at $3\text{ kg CO}_2\text{ equiv. per kg production}$.^[35,36] Recovering carbon fibers from CFRC wastes could help compensate for

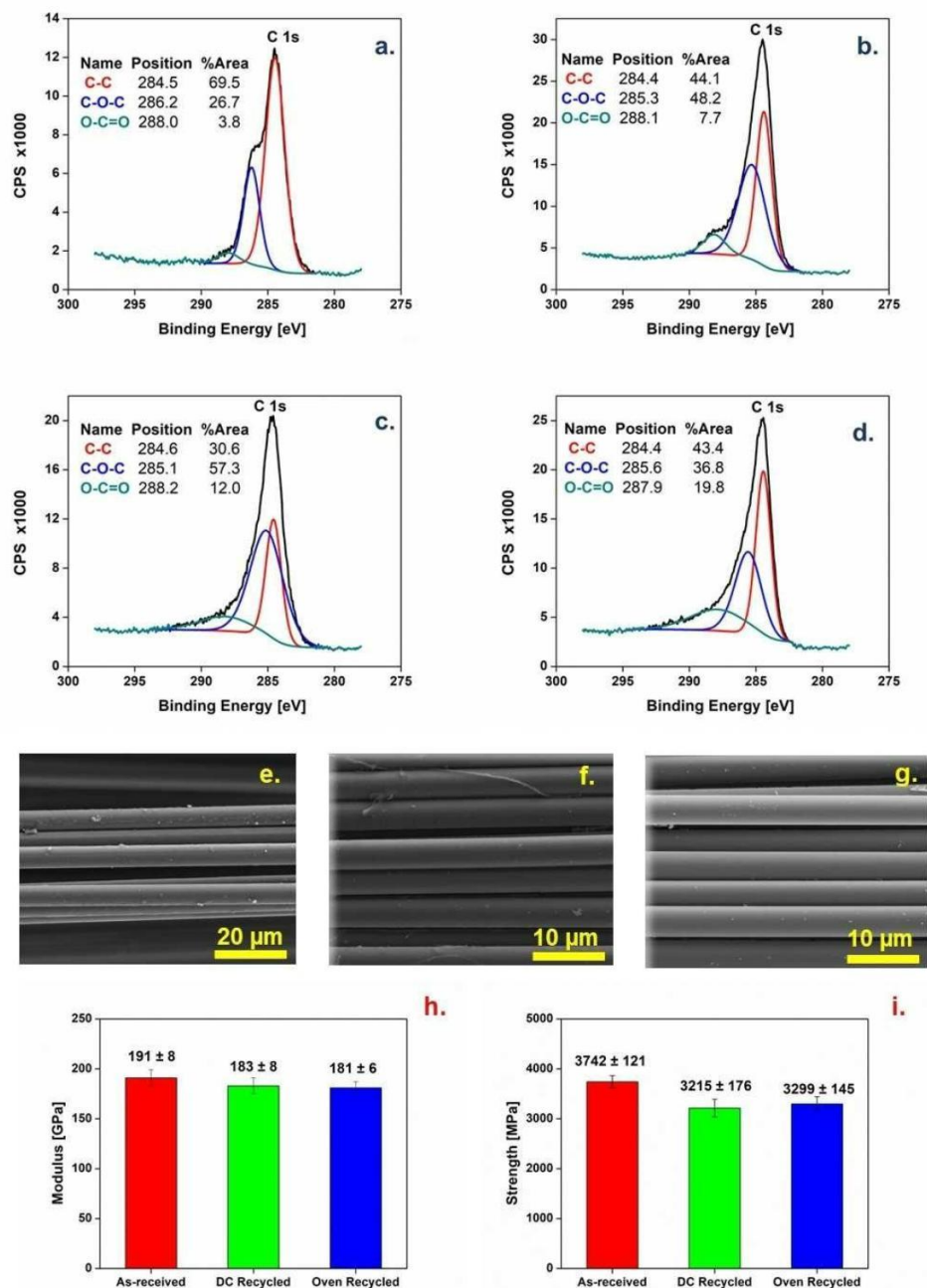


Figure 3. Deconvoluted XPS spectra of (a) as-received IM7 fibers, (b) de-sized IM7 fibers, (c) DC-recycled IM7 fibers, (d) oven-recycled IM7 fibers. SEM images of (e) as-received IM7 fibers, (f) DC-recycled IM7 fibers, and (g) oven-recycled IM7 fibers. (h) Modulus of elasticity and (i) strength of single fibers of as-received IM7 CFs, DC-recycled IM7 CFs and oven-recycled IM7 CFs.

these production impacts and reduce the greenhouse emissions from incineration. Additionally, recycling of carbon fibers from CFRCs is of growing importance on account of environmental legislation becoming stricter by the day. Thus, it is imperative to adopt a sustainable method to recycle carbon fibers. In this work, we have successfully established DC heating as an effective methodology to recycle continuous carbon fibers from end-of-life composites.

To demonstrate applications of recycled carbon fibers, we fabricated rCFRCs, which were 4-ply thick with in-plane dimensions 70 mm × 10 mm using the same resin system as the initial composites (Figure 4a). The mechanical properties of composites made using fibers recycled via both DC heating and conventional pyrolysis were compared. A composite of similar dimensions made from as-received IM7 fibers was used as a control specimen. Composites made using DC-recycled and

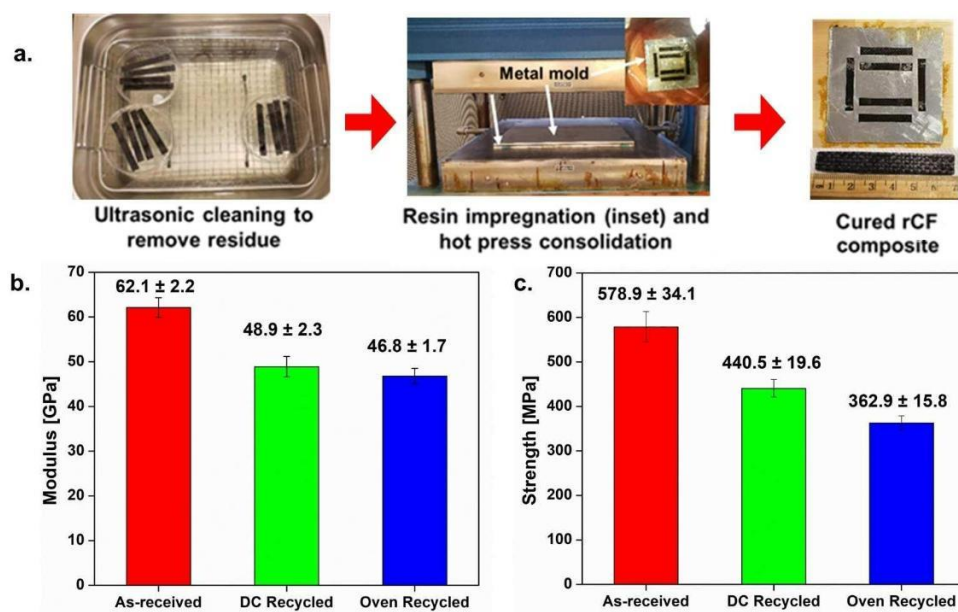


Figure 4. (a) Fabrication of rCFRC. (b) Modulus of elasticity and (c) strength of single fibers of as-received IM7 CFs, DC-recycled IM7 CFs and oven-recycled IM7 CFs.

oven-recycled fibers had similar modulus values; however, these values are about 20% lower than the modulus of composite made using as-received fibers (Figure 4b). The tensile strength of composites made from DC-recycled fibers was measured to be about 440.5 GPa, which is higher than the value observed for composites made using oven-recycled fibers (around 362.9 GPa). We observed drops of approximately 20% and 37% in tensile strengths for the composites made using DC heating, and oven heating recycled fibers, respectively, compared to the control specimen (Figure 4c).

The drop in mechanical properties of DC-recycled rCFRCs when compared to composites made using as-received fibers may be attributed to the fact that thermal treatment (both DC heating and oven pyrolysis) removes the sizing of carbon fibers. The sizing is a highly proprietary coating on virgin carbon fibers, which enhances cross-linking between fiber and matrix

and strengthens the fiber-matrix interface; thus, its absence in recycled fibers affects the modulus and strength of the final cured part. Reapplying the sizing on these recycled fibers could likely improve the mechanical properties of the resulting rCFRCs; however, due to its unknown nature,^[37] re-sizing can only be carried out by the fiber manufacturer. Composites made of fibers recycled using DC heating fared significantly better when compared against composites made using conventionally recycled fibers.

Next, the scalability of this methodology was analyzed to investigate the potential transfer of technology from the laboratory to the industry. The power and energy required to recycle composites of varying sizes and weights were measured. Power required for recycling was plotted against the composite volume in Figure 5a; the plot follows a sub-linear relationship. Moreover, it can be seen that the energy required per unit mass

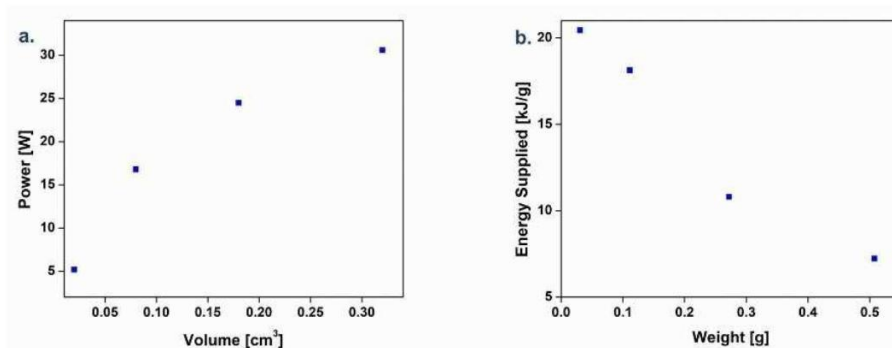


Figure 5. (a) Power required vs. volume of composite to maintain the sample at $T = 400^\circ\text{C}$. (b) Energy required per unit weight vs. weight of the sample to maintain $T = 400^\circ\text{C}$ for 10 min.

for recycling decreases with an increase in sample weight (Figure 5b). Thus, this methodology of recycling continuous carbon fibers can be potentially ramped up to a commercial scale without an extreme rise in energy usage.

Conclusions

We have successfully recycled continuous carbon fibers from end-of-life thermoset composites using direct current (DC)-induced Joule heating; these recycled fibers could be potentially reused to make composites for various multi-functional applications. The surface morphology and chemistry of as-received carbon fibers and DC-recycled carbon fibers are comparable, with the same types of functional groups found on the surfaces of both types of fibers. While the elastic modulus of as-received and DC-recycled fibers are similar, there is an around 10–15% decrease in tensile strength of the DC-recycled fibers when compared to the as-received fibers. DC-recycled fibers were reused successfully to fabricate recycled carbon fiber composites (rCFRCs), with a loss of about 20% in mechanical properties. We have also established that this method has the potential to be scaled up to the industrial level. The production of virgin carbon fibers causes large CO₂ emissions and is also an energy-intensive process.^[36] Thus, using the current method proposed here, we demonstrate the recycling and reuse of carbon fibers which could diminish the environmental impact of using carbon fiber reinforced composites (CFRCs).

Experimental Section

Materials

For this study, thermoset composites with IM7 (Hexcel, Stamford, CT) carbon fibers were used. The first type of composite had unidirectional carbon fibers impregnated with epoxy made from EPON 862 epoxide cured with Epikure W (Miller-Stephenson, Danbury, CT); the second composite used in this study had the same matrix system with the cross-weave IM7 carbon fibers cured with the same matrix (Figure S7). Both composites were 4 layers thick and were cured at 121 °C for 1 h, followed by 177 °C for 2.5 h using a heated platen press.

Thermogravimetric analysis

TGA ramp experiments were performed in the air for cross-weave and unidirectional composites to determine the degradation temperature of the matrix; the temperature was ramped from room temperature to 600 °C at a rate of 10 °C min⁻¹. Next, isothermal TGA experiments were performed at the degradation temperature determined from the temperature run; the sample was heated rapidly to the degradation temperature and held isothermally for 10 min. The residual weight at the end of each run was noted.

DC heating

The DC heating setup used for recycling carbon fibers is shown in Figure 2a. The CFRC composite was placed on a ceramic tile and

copper tape was attached to the ends of the composite; silver paste was used to ensure proper electrical contact between the tape and the composite. Alligator clips were used to connect the copper tapes to a direct current power source. The DC supply voltage was modulated manually to ramp up the sample to its target temperature and maintain it for the desired residence time. The temperature was monitored using a FLIR A655sc thermal camera.

X-ray photoelectron spectroscopy

XPS was performed on carbon fibers using an Omicron X-ray photoelectron spectrometer employing an Mg-sourced X-ray beam at 15 kV with aperture 3. The scan spectra were recorded in the range 0–1100 eV. The carbon (C), nitrogen (N), and oxygen (O) traces were scanned. The binding energy was calibrated by referring to the C 1s peak at 284.8 eV. For this characterization, some as-received fibers were thermally treated at 450 °C for 15 min to remove the proprietary coating or 'sizing'; these fibers are referred to as "de-sized" fibers. XPS scans of as-received carbon fibers, de-sized carbon fibers, oven-recycled carbon fibers, and DC-recycled carbon fibers were compared.

Scanning electron microscopy

The surface morphologies of the as-received, DC-recycled and oven-recycled carbon fibers were observed using a scanning electron microscope (Tescan LYRA-3 Model GMH Focused Ion Beam Microscope) to investigate the degree of degradation of the resin matrix and potential damage to the fiber surfaces. The operating accelerating voltage was 10 kV.

Single fiber testing

Unidirectional carbon fibers extracted from composites thermally treated using DC heating and conventional oven pyrolysis were used for single fiber mechanical testing. A paper sample tab with a gauge length of 10 mm was used to mount the samples to the tensile stage, as seen in Figure S8. The strain rate was set to be 0.5 mm s⁻¹, and a minimum of 20 samples were tested from each fiber type. Modulus and tensile strength were measured for each fiber type using the data from this experiment. As-received unidirectional IM7 fibers were used as the control specimen for this experiment.

Matrix reinfiltration and mechanical testing of composites

After DC heating or oven pyrolysis, the laminas in 4-ply cross-weave composites were separated for cleaning. The laminas were kept in an ultrasonic bath of deionized water for 15 min at room temperature to remove traces of the residual epoxy. Once dried, an aluminum mold with in-plane dimensions of 70.5 mm × 10.5 mm was used for making composites from the recycled fibers. Layers (or lamina) of the fibers were laid one by one, and each layer was impregnated with the same resin system used to make the original

composite. The curing cycle consisted of keeping the system at 121 °C for 1 h, followed by 177 °C for 2.5 h in a heated platen press. Composites with dimensions of 70 mm × 10 mm made of fibers recycled using DC heating or oven pyrolysis were mechanically tested to measure tensile strength and modulus. An Instron model #2630-101 frame with a 50 kN load cell was used for these tests; the displacement rate was set at 1.27 mm min⁻¹ for all tests. Composite made using as-received IM7 weave was used as the control specimen for these tests.

Acknowledgments

The authors would like to thank the Materials Characterization Facility (RRID:SCR_022202) at Texas A&M University for SEM and XPS. The authors thank the Soft Matter Facility (RRID:SCR_022482) at TAMU for TGA. JT and AV would like to thank the Mechanical Engineering Composite Shop at the University of Washington for composite fabrication. The authors also thank Dr. Carolyn Long, Texas A&M University, for her assistance with creating Figure 1. The authors thank Tommy Chen, Stan Ng, and Eva Thorn from NAVAIR for their helpful comments. The work was supported in part by United States Naval Air Systems Command (NAVAIR) under contract N68335-21-C-0494.

Conflict of Interest



there is pending IP on the contents of this manuscript

Data Availability Statement

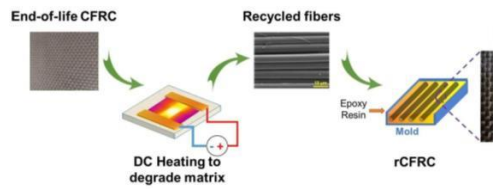
Research data are not shared.

Keywords: composite scrap · direct current (DC) · Joule heating · recycled carbon fiber composites (rCFRCs) · scale up

- [1] N. Vijay, V. Rajkumara, P. Bhattacharjee, *Procedia Environ. Sci.* **2016**, *35*, 563–570.
- [2] V. P. McConnell, *Reinf. Plast.* **2010**, *54*, 33–37.
- [3] Y. Yang, R. Boom, B. Irion, D.-J. van Heerden, P. Kuiper, H. de Wit, *Chem. Eng. Process.* **2012**, *51*, 53–68.
- [4] S. Pompidou, M. Prinçaud, N. Perry, D. Leray, *ASME 2012 11th Biennial Conference on Engineering Systems Design and Analysis* **2012**.
- [5] C. A. Navarro, C. R. Giffin, B. Zhang, Z. Yu, S. R. Nutt, T. J. Williams, *Mater. Horiz.* **2020**, *7*, 2479–2486.
- [6] K. Yu, Q. Shi, M. L. Dunn, T. Wang, H. J. Qi, *Adv. Funct. Mater.* **2016**, *26*, 6098–6106.
- [7] Y. Liu, M. Farnsworth, A. Tiwari, *J. Cleaner Prod.* **2017**, *140*, 1775–1781.
- [8] S. Pimenta, S. T. Pinho, *Waste Manage.* **2011**, *31*, 378–392.
- [9] F. Meng, E. A. Olivetti, Y. Zhao, J. C. Chang, S. J. Pickering, J. McKechnie, *ACS Sustainable Chem. Eng.* **2018**, *6*, 9854–9865.
- [10] L. Giorgini, T. Benelli, L. Mazzocchetti, C. Leonardi, G. Zattini, G. Minak, E. Dolcini, M. Cavazzoni, I. Montanari, C. Tosi, *Polym. Compos.* **2015**, *36*, 1084–1095.
- [11] D. Borjan, Z. Knez, M. Knez, *Materials* **2021**, *14*, 4191.
- [12] G. Oliveux, L. O. Dandy, G. A. Leeke, *Prog. Mater. Sci.* **2015**, *72*, 61–99.
- [13] J. Chen, J. Wang, A. Ni, *J. Reinf. Plast. Compos.* **2019**, *38*, 567–577.
- [14] C.-K. Lee, Y.-K. Kim, P. Pruitichaiwiboon, J.-S. Kim, K.-M. Lee, C.-S. Ju, *Transp. Res. D Transp. Environ.* **2010**, *15*, 197–203.
- [15] S. Verma, B. Balasubramaniam, R. K. Gupta, *Curr. Opin. Green Sustain. Chem.* **2018**, *13*, 86–90.
- [16] J. Palmer, O. R. Ghita, L. Savage, K. E. Evans, *Composites Part A* **2009**, *40*, 490–498.
- [17] J. Jiang, G. Deng, X. Chen, X. Gao, Q. Guo, C. Xu, L. Zhou, *Compos. Sci. Technol.* **2017**, *151*, 243–251.
- [18] S. R. Naqvi, H. M. Prabhakara, E. A. Bramer, W. Dierkes, R. Akkerman, G. Brem, *Resour. Conserv. Recycl.* **2018**, *136*, 118–129.
- [19] P. T. Williams, A. Cunliffe, N. Jones, *J. Energy Inst.* **2005**, *78*, 51–61.
- [20] K. Ogi, T. Nishikawa, Y. Okano, I. Taketa, *Adv. Compos. Mater.* **2007**, *16*, 181–194.
- [21] T. Y. Wu, W. Q. Zhang, X. Jin, X. Y. Liang, G. Sui, X. P. Yang, *RSC Adv.* **2019**, *9*, 377–388.
- [22] I. Okajima, M. Hiramatsu, Y. Shimamura, T. Awaya, T. Sako, *J. Supercrit. Fluids* **2014**, *91*, 68–76.
- [23] R. Piñero-Hernanz, J. García-Serna, C. Dodds, J. Hyde, M. Poliakov, M. J. Cocero, S. Kingman, S. Pickering, E. Lester, *J. Supercrit. Fluids* **2008**, *46*, 83–92.
- [24] R. Piñero-Hernanz, C. Dodds, J. Hyde, J. García-Serna, M. Poliakov, E. Lester, M. J. Cocero, S. Kingman, S. Pickering, K. H. Wong, *Composites Part A* **2008**, *39*, 454–461.
- [25] N. T. Tran, B. A. Patterson, A. G. Kolodziejczyk, V. M. Wu, D. B. Knorr, *Langmuir* **2019**, *35*, 12374–12388.
- [26] C. W. Visser, R. Pohl, C. Sun, G. W. Roemer, B. H. in 't Veld, D. Lohse, *Adv. Mater.* **2015**, *27*, 4087–4092.
- [27] L. O. Meyer, K. Schulte, E. Grove-Nielsen, *J. Compos. Mater.* **2009**, *43*, 1121–1132.
- [28] L. Giorgini, T. Benelli, L. Mazzocchetti, C. Leonardi, G. Zattini, G. Minak, E. Dolcini, C. Tosi, I. Montanari, *AIP Conf. Proc.* **2014**, *1599*, 354–357.
- [29] K.-L. Lam, A. O. Oyedun, K.-Y. Cheung, K.-L. Lee, C.-W. Hui, *Chem. Eng. Sci.* **2011**, *66*, 6505–6514.
- [30] L. Jiang, C. A. Ulven, D. Gutschmidt, M. Anderson, S. Baló, M. Lee, J. Vigness, *J. Appl. Polym. Sci.* **2015**, *132*, 42658.
- [31] S. Q. Hao, L. Z. He, J. Q. Liu, Y. H. Liu, C. Rudd, X. L. Liu, *Polymer* **2021**, *13*, 1231..
- [32] M. Anas, M. M. Mustafa, D. G. Carey, A. Sarmah, J. J. LeMonte, M. J. Green, *Carbon* **2021**, *174*, 518–523.
- [33] Y. Cheng, G. Cui, C. H. Liu, Z. T. Liu, L. G. Yan, B. Y. Liu, H. Yuan, P. C. Shi, J. Jiang, K. W. Huang, K. Wang, S. T. Cheng, J. L. Li, P. Gao, X. F. Zhang, Y. Qi, Z. F. Liu, *Adv. Funct. Mater.* **2022**, *32*, 2103493..
- [34] B. Deng, D. X. Luong, Z. Wang, C. Kittrell, E. A. McHugh, J. M. Tour, *Nat. Commun.* **2021**, *12*, 5794..
- [35] P. A. Vo Dong, C. Azzaro-Pantel, A.-L. Cadene, *Resour. Conserv. Recycl.* **2018**, *133*, 63–75.
- [36] S. Das, *Int. J. Life Cycle Assess.* **2011**, *16*, 268–282.
- [37] S. S. Pawar, S. A. Hutchinson, D. J. Eyckens, F. Stojcevski, D. J. Hayne, T. R. Gengenbach, J. M. Razal, L. C. Henderson, *Compos. Sci. Technol.* **2022**, *220*, 109280.

Manuscript received: May 24, 2022
 Revised manuscript received: August 30, 2022
 Accepted manuscript online: August 30, 2022
 Version of record online:  

RESEARCH ARTICLE



Carbon fiber recycling: A direct current (DC) power supply is used to induce electric currents in an end-of-life carbon fiber composite. Joule heating of the conductive fibers degrade the surrounding epoxy

matrix, thus allowing for recycling of carbon fibers from the composites. These reclaimed fibers are re-infiltrated with epoxy and cured to make recycled carbon fiber composites.

*A. Sarmah, S. Sarikaya, J. Thiem, S. T. Upama, A. N. Khalfaoui, S. S. Dasari, K. Arole, Dr. S. A. Hawkins, Prof. M. Naraghi, Dr. A. Vashisth, Prof. M. J. Green**

1 – 8

Recycle and Reuse of Continuous Carbon Fibers from Thermoset Composites Using Joule Heating

